RADC-TR-76-230
Final Technical Report
July 1976

COAT/TARGET-SIGNATURE INTERACTIONS

Hughes Research Laboratories

Sponsored By
Defense Advanced Research Projects Agency
ARPA Order No. 1279

ROME AIR DEVELOPMENT CENTER
AIR FORCE SYSTEMS COMMAND
GRIFFISS AIR FORCE BASE, NEW YORK 13441

This report has been reviewed by the RADC Information Office (OI) and is releasable to the National Technical Information Service (NTIS). At NTIS it will be releasable to the general public including foreign nations.

This report has been reviewed and is approved for publication.

Robert F. Ogrodnik

ROBERT F. OGRODNIK
Project Engineer

Do not return this copy. Retain or destroy.

COAT/TARGET-SIGNATURE INTERACTIONS

M. E. Pedinoff
S. A. Kokorowski
J. E. Pearson

Contractor: Hughes Aircraft Laboratories
Contract Number: F30602-76-C-0021
Effective Date of Contract: 1 August 1975
Contract Expiration Date: 30 June 1976
Short Title of Work: COAT/Target-Signature Interactions
Program Code Number: 6E20
Period of Work Covered: Aug 75 - Feb 76

Principal Investigators: M. E. Pedinoff, J. E. Pearson &
S. A. Kokorowski
Phone: 213 456-6411, Ext. 283

Project Engineer: Robert F. Ogrodnik
Phone: 315 330-4306

This research was supported by the Defense Advanced Research Projects Agency of the Department of Defense and was monitored by Robert F. Ogrodnik (OCTM), Griffiss AFB NY 13441.

UNCLASSIFIED

SECURITY CLASSIFICATION OF THIS PAGE *(When Date Entered)*

REPORT DOCUMENTATION PAGE	READ INSTRUCTIONS BEFORE COMPLETING FORM
1. REPORT NUMBER: RADC-TR-76-230	2. GOVT ACCESSION NO.
	3. RECIPIENT'S CATALOG NUMBER
4. TITLE *(and Subtitle)*: COAT/TARGET-SIGNATURE INTERACTIONS	5. TYPE OF REPORT & PERIOD COVERED: Final Technical Report. 1 Aug 75 — 1 Feb 76
	6. PERFORMING ORG. REPORT NUMBER: N/A
7. AUTHOR(s): M. E. Pedinoff, S. A. Kokorowski, and J. E. Pearson	8. CONTRACT OR GRANT NUMBER(s): F30602-76-C-0021; ARPA Order-1279
9. PERFORMING ORGANIZATION NAME AND ADDRESS: Hughes Research Laboratories, 3011 Malibu Canyon Road, Malibu CA 90265	10. PROGRAM ELEMENT, PROJECT, TASK AREA & WORK UNIT NUMBERS: 62301E, 12790020
11. CONTROLLING OFFICE NAME AND ADDRESS: Defense Advanced Research Projects Agency, 1400 Wilson Blvd, Arlington VA 22209	12. REPORT DATE: July 1976
	13. NUMBER OF PAGES: 94
14. MONITORING AGENCY NAME & ADDRESS *(if different from Controlling Office)*: Rome Air Development Center (OCTM), Griffiss AFB NY 13441	15. SECURITY CLASS. *(of this report)*: UNCLASSIFIED
	15a. DECLASSIFICATION/DOWNGRADING SCHEDULE: N/A

16. DISTRIBUTION STATEMENT *(of this Report)*
Approved for public release; distribution unlimited.

16 AF-1279 17 127900

17. DISTRIBUTION STATEMENT *(of the abstract entered in Block 20, if different from Report)*
Same

18. SUPPLEMENTARY NOTES

RADC Project Engineer:
Robert F. Ogrodnik (OCTM)

19. KEY WORDS *(Continue on reverse side if necessary and identify by block number)*
COAT, Speckle, Target Signature Effects, Laser Phased Arrays, Active Optics, Adaptive Systems.

20. ABSTRACT *(Continue on reverse side if necessary and identify by block number)*
Amplitude modulation effects which can occur when target return speckle patterns move by a receiver aperture, have been studied in adaptive optical systems that use multidither coherent optical adaptive techniques (COAT). Good agreement is found between experimental, analytical, and computer simulation studies made to characterize the degree to which COAT systems can be affected by speckle. Both experimental and computer simulation results show that in the worst-case, the convergence-level (Strehl ratio) of an 18-element COAT system is reduced to 30% of that obtained with no spurious speckle modulations.

DD FORM 1 JAN 73 1473 EDITION OF 1 NOV 65 IS OBSOLETE 1 UNCLASSIFIED

SECURITY CLASSIFICATION OF THIS PAGE *(When Data Entered)*

CONTINUED

172600

Calculations using an analysis developed here, predict an average convergence level of 0.18, in reasonable agreement with experiment, but somewhat pessimistic.

In the presence of speckle noise, the COAT system convergence rate is unaffected, as is the convergence level until it reaches the "average" level that is set by the speckle noise. The convergence level then oscillates in a random fashion between well-defined maximum and minimum values. For any given multidither COAT system, we have developed analytical and computer simulation tools that can accurately predict the average convergence level and oscillation extremes once the power spectrum of speckle-induced modulations is known.

We have observed that reducing the servo gain (bandwidth) reduces the effect of speckle modulations nearly to zero, but at the cost of increased convergence time. We have also found that a hard limiter (clipper) reduces the speckle-induced degradations, but with no loss in convergence time. The common-channel AGC parameters also play an important role.

Compensation for turbulence and blooming distortions was studied experimentally, with and without speckle effects. Some compensation is always observed, even with strong speckle effects but peak target irradiance is always less when strong speckle modulations occur.

We conclude that speckle effects can seriously degrade the performance of multi-dither COAT systems, but that the amount of degradation depends strongly on target parameters (range, surface roughness, rotation rate) and on COAT system parameters (servo details and parameters, laser bandwidth, etc.). Our data indicates that there is a reasonably narrow "window" of target motion rates that can produce serious COAT performance degradation, all other parameters held constant. Rates faster or slower than those within the window produce minimal speckle effects. Carefully collected data on speckle pattern returns from realistic targets and with realistic illumination functions is needed along with an assessment of how probable the "degradation window" is for high power COAT application scenarios. If strong degradations are likely to occur, then advanced techniques should be pursued that can minimize speckle effects within a multidither servo.

PREFACE

This report was prepared by Hughes Research Laboratories, Malibu, California under Contract F30602-76-C-0021. It summarizes the results of a six-month experimental and analytical study of the interaction between multidither COAT systems and target-produced amplitude modulations in a COAT receiver. An interim report (Dec. 1975) describes the early contract progress in detail. This report deals mainly with results obtained during the last half of the contract, while summarizing the entire contract. The principal scientist is Dr. James E. Pearson and the principal investigators are Dr. Melvin E. Pedinoff and Mr. Stan A. Kokorowski. This project is a part of the Adaptive Optics program in the Opto-Electronics Department, managed by Dr. Viktor Evtuhov, at the Hughes Research Laboratories.

TABLE OF CONTENTS

LIST OF ILLUSTRATIONS

LIST OF ILLUSTRATIONS (Continued)

SUMMARY

The objectives of this program are threefold: (1) to determine the characteristics of receiver modulations produced by backscatter from realistic targets that interfere with the proper operation of a multidither COAT system and to assess the degradation they produce in COAT system convergence and performance; (2) to develop a unified theory of the interaction between a multidither COAT system and target-speckle induced receiver modulations; (3) to determine an optimum COAT system design that is insensitive to speckle-induced receiver modulations and to define the critical design parameters. This report summarizes the entire contract work performed from 1 August 1975 to 1 February 1976, concentrating mainly on the results obtained from 31 October 1975 to 1 February 1976.

We have experimentally studied the speckle patterns generated by scaled, realistic target models consisting of metallized or painted spheres, cylinders, and cones using a helium-neon (6328 Å) laser and a target-speckle measurement apparatus specifically assembled for this program. Target signatures were recorded with two receiver aperture diameters, one equal to the transmitter diameter and one equal to one-third of the transmitter diameter. The larger aperture size significantly reduced the observed speckle contrast ratio and reduced the amplitude of the higher speckle spatial frequency components.

Speckle pattern data have been reduced using a fast-Fourier-transform to obtain spatial frequency spectra. The same spectrum is obtained by translating the receiver as by rotating the target. Target speckle signatures taken with most of the metallized target shapes are very similar. The maximum contrast ratio* observed in all of the experiments was 0.89 with the most commonly observed maximum contrast ratio being 0.56.

*Defined as $(I_{max} - I_{min})/(I_{max} + I_{min})$, where I = observed irradiance.

Real-time spectrum analyzer spectra obtained by rapid rotation of the targets are identical to spatial frequency spectra obtained by performing a fast-Fourier-transform (FFT) on the speckle pattern. data. Increasing the target rotation speed caused the speckle spectrum to broaden toward high frequencies in agreement with the FFT spatial frequency results. This result is useful for explaining the effect of target rotation on COAT system convergence level. The speckle signatures produced by rotation of the metallized targets are very similar to those produced on an earlier program (Contract F30602-75-C-0001) by rotating scotchlite targets.

Very little difference in speckle properties was observed with spherical, conical, or cylindrical targets. Consequently, the metallized spherical target was used as a vehicle to test COAT system performance because it was the most convenient experimentally.

Following the detailed measurements on speckle patterns, the spherical target was used as a target in the DARPA/RADC 18-channel COAT system. The system convergence behavior was measured as a function of target rotation speed for several target orientations. Significant degradation of the converged power to a normalized level of $P = 0.31$ was observed when the target rotated at $\Omega = 2\pi$ rad/sec about an axis at 90° to the incident beam ($P = 1.0$ at $\Omega = 0$). Slower or faster rotation rates produced less degradation. When the COAT system feedback loop gain was reduced by 15 dB (rotation optimization), the converged power level was 0.93. Similar experiments carried out with the target rotation axis at 45° to the incident beam yielded strong degradation ($P = 0.50$) and good recovery ($P = 0.80$) of COAT convergence for the high loop gain (static optimization) and low loop gain (rotation optimization) cases, respectively. When the target axis was parallel to the laser axis (0°), negligible degradation of system convergence was observed, even with high loop gain.

The convergence time of the system was, of course, affected by the loop gain. In the presence of speckle modulation, the COAT system oscillates between two levels whose mean decreases as the speckle modulation power in the dither band increases. The convergence time

to this mean level for the condition of high loop gain is essentially unaffected by the modulations. When the system loop gain is reduced (ΔG = -15 dB) to counteract the effects of speckle modulation, however, the convergence time increases at most by a factor of 6 and on the average by a factor of 4. (The product of loop gain and convergence time is approximately constant.)

Although most of the experimental measurements were made with no propagation distortions, we have also investigated the ability to perform turbulence and blooming compensation in the presence of speckle. The distortions existed only on the outgoing beam path, however, and thus did not affect the speckle itself in any way. In general, we find that the existence of speckle modulations does not significantly remove the COAT system's ability to correct for blooming and turbulence, although the amount of correction and the peak target irradiance are usually both less when speckle effects are present. The degree of reduction in compensation depends on the amount of speckle-induced power within the COAT system dither band as might be expected. In each case studied, the COAT system could not improve the beam strehl ratio over that set by the speckle. For example, if speckle alone produces a strehl ratio of 0.3, and turbulence alone (when uncorrected) produces a strehl ratio of 0.4, the strehl ratio of the beam with both effects is 0.3. If the speckle strehl ratio is 0.6, however, then the turbulence-plus-speckle ratio will be somewhere between 0.4 and 0.6, usually closer to the 0.6 level as set by the speckle.

Analytical work conducted throughout this program consisted in part of computer simulation studies of COAT system convergence in the presence of broadband speckle-like noise. Computer simulations of multidither COAT performance have been made using both an ad hoc "speckle" spectrum and theoretical target-speckle data generated by the General Research Corporation (GRC). The ad hoc spectrum consisted of 23 discrete frequencies of random amplitude and phase placed within the servo bandwidth of each of 18 COAT control channels. The data supplied by GRC were calculated using a full diffraction calculation and the following parameters: target-range = 2 km, shape = 10 cm diameter segment of 1 m radius sphere, illumination = uniform, material = pyroceram, assumed completely random in phase reflection; other, wavelength = 10.6 μm, annular receiver (1.2 m x 1.0 m diameters) about a 20 cm diameter transmitter.

Both types of modulation, applied as multiplicative receiver noise, gave qualitatively similar results. That is, as the noise power increased, the average convergence level decreases and the COAT system convergence level (strehl ratio) oscillates between two well-defined levels. Qualitatively, this observation also agrees with experiment. Three cases were run with GRC-supplied data corresponding to target rotations about an axis perpendicular to the illumination beam direction of $\Omega = 0.4$, 2, and 10 rad/sec. The average convergence levels from these runs were 0.74, 0.32, and 0.51, compared to 0.95 for no speckle modulations.

An analysis has been developed to aid in understanding the experimental and simulation data and to provide a means for predicting COAT system performance in the presence of speckle modulations. The analysis includes a statistical model of a multidither COAT system and incorporates speckle modulations as a noise source. The analysis defines the system performance in terms of two parameters: C_S, called the "speckle coefficient" and ρ', the ratio of the average dither signal power to the average speckle modulation power after synchronous detection. The quantity C_S is proportional to the square-root of the total speckle-produced power within a servo bandwidth around all the dither frequencies and can have a maximum value of $\sqrt{2} \approx 0.707$.

The analysis predicts that the observed maximum and minimum convergence levels are defined by $\rho' = 0.5$ and $\rho' = 2.0$, with $\rho' = 1.0$ being the average. It also says that the $\Omega = 2.0$ rad/sec case supplied by GRC does not represent the theoretical worst-case since $C_S = 0.24$ for that scenario (although given the COAT parameters, it is the worst case of the ones studied). Very good qualitative agreement has been obtained between the analysis and computer simulation data and with experimental data. Quantitatively, the experimental and simulation data agree when the parameters are scaled properly. The analysis, however, is somewhat pessimistic in its predictions. For example, the $\Omega =$ 2 rad/sec GRC case most closely scales to a laboratory experiment where $\Omega = 2\pi$ rad/sec. The experimental strehl ratio is 0.31, the computer simulation result is 0.30, and the analysis predicts 0.18.

This program has thus established both experimentally and by computer simulation that speckle effects can significantly degrade the performance of a multidither COAT system and we have developed analytical and computer simulation tools that enable us to predict COAT system performance beyond the particular 18-channel system studied here. We have also established, however, that the degradation produced by speckle depends strongly on the speckle contrast ratio and on the rate at which the speckle pattern moves by the COAT receiver. These parameters in turn are sensitive functions of the target shape, size, surface roughness and motion as well as of the target range and the illumination laser bandwidth. The COAT system parameters also play an important role. For example, we have noted that lower gain (lower servo bandwidth) reduces speckle effects; we have also established that a higher dither modulation index (up to a point) and the presence of a hard limiter (clipper) in the servo improve performance in the presence of speckle.

Additional work still needs to be done to quantitatively establish the effect of modulation index, of the number of channels, and of allowing the speckle itself to change as the COAT convergence level changes. The effect of servo bandwidth variation with convergence level has not been included in the analysis and such an addition would increase its usefulness. Perhaps most important is the need to establish what scenarios can produce significant speckle modulations that fall with the COAT system dither band and how probable is the occurrence of such scenarios. If the probability of occurrence is high, then advanced techniques for reducing the degrading effects of speckle should be pursued.

SECTION I

INTRODUCTION

A. PROGRAM OBJECTIVES

The overall purpose of this program is to produce a consistent, unified theory on multidither COAT/target interactive effects that correlate experimental data with analytical models. Specifically there are three primary objectives. The first objective is to determine what kind of modulations interfere with the proper operation of a multidither COAT system. The significant parameters of the modulation are contrast ratio and frequency spectrum. The second objective is to determine the characteristics of receiver modulations produced by backscatter from real targets in expected operational scenarios; that is, to determine which scenarios can produce the modulations which will affect the COAT system. The third objective is to determine an optimum COAT system design that is insensitive to speckle-induced receiver modulations and to define the critical design parameters.

B. RESEARCH PROGRAM PLAN

The 18-element multidither COAT system developed and tested on DARPA/RADC Contract F30602-73-C-0248 is used for laboratory experiments on this program, which is an in-depth investigation of speckle phenomena in multidither COAT systems.

The research program for this contract, illustrated in Table 1, runs from 1 August 1975 to 1 February 1976. Because of ongoing measurements on the COAT Measurements and Analysis program (Contract F30602-75-C-0001), a separate target-speckle measurement apparatus was used. The apparatus included a helium-neon 6328 Å laser for target illumination and a nearly collinear receiver system for target backscatter characterization studies. Theoretical speckle simulation studies were also conducted.

TABLE 1. COAT/TARGET-SIGNATURE RESEARCH PROGRAM PLAN

5215-1

TASK	1975					1976	
	A	S	O	N	D	J	F
TARGET BACKSCATTER MEASUREMENTS	■	■	■				
COAT SYSTEM MEASUREMENTS				■	■	■	■
1. INDUCED MODULATIONS IN RECEIVER: NO COAT CORRECTION, NO DISTORTIONS				■			
2. COAT CORRECTION, SCALED TARGET SCENARIOS, TURBULENCE AND BLOOMING						■	■
ANALYTICAL STUDIES	■	■	■	■	■	■	■

Some of the computer simulation work used target speckle-signatures generated by General Research Corporation (GRC) under Contract F3602-75-C-0086. The program is divided into three tasks: Target Backscatter Measurements, COAT System Measurements, and Analytical Studies. Task 1 represents the acquisition and characterization of targets and target speckle data not previously available to the program. Task 2 determines COAT system performance in the presence of turbulence, blooming, and speckle noise modulation from these targets. Task 3 is a computer simulation study designed to corroborate or predict the experimental findings. Preliminary results from Tasks 1 and 3 are reported in the Interim Report on this contract, dated December 1975.

C. REPORT ORGANIZATION

This report serves two functions: (1) it presents the accomplishments of the second half of this program, and (2) it summarizes the principal accomplishments of the entire contract. The report is thus both a second half technical report and a final technical report.

Section II reviews the target speckle characterization accomplishments obtained during the first half of this program and presents complete data on the performance of COAT systems in the presence of speckle; blooming and speckle; and blooming, turbulence, and speckle.

Section III summarizes the results of the analytical efforts directed toward investigating complex target effects (speckle) in COAT systems. The data obtained were primarily obtained by computer simulations using target signatures generated by GRC. Comparisons are made between analytical, computer simulation, and experimental results.

Section IV summarizes the principal results of the contract and the conclusions that can be drawn from the work. The implications for additional research that should follow this work are presented.

An appendix contains a development of the theoretical model of the effect of speckle on a COAT system, and a statistical model of a multidither COAT system. In combination, these analytical models provide a experimentally verified method for predicting COAT

convergence behavior in the presence of speckle modulation. Computer simulation results using artificial speckle modulation are also in good agreement with the analytical predictions. This appendix forms a basis for understanding the computer simulation results presented in Section III.

SECTION II

EXPERIMENTAL TECHNICAL ACCOMPLISHMENTS

A. EXPERIMENTAL TARGET SPECKLE MEASUREMENTS

In the first part of the experimental study reported in the Interim Technical Report, we characterized the general properties of speckle patterns associated with various targets to identify those most likely to produce degradation in COAT system performance. Speckle pattern measurements were obtained on targets consisting of glass spheres, cones, and cylinders that were either electroplated with nickel or painted to simulate the effect of real target surfaces. The static speckle characteristics were measured in the apparatus shown in Figure 1. The output of a 6328 Å helium-neon laser was spatially filtered and expanded with a standard telescope. The beam was truncated at its full width, half maximum (FWHM) by an iris, and then recollimated to 0.15 mm diameter (FWHM) with a second telescope. The beam then illuminated the target at a distance of about two meters from the exit pupil. Energy backscattered from the target was reflected by a mirror through a pinhole iris into a photomultiplier (PMT) detector. Two irises, 0.15 mm and 0.05 mm in diameter, were available during the experiment so that speckle data could be recorded when the receiver and transmitter were of equal diameter ($D_T = D_R = 0.15$ mm) and when the receiver diameter was equal to one third the transmitter diameter ($D_T = 0.15$ mm, $D_R = 0.05$ mm). The target stage was rotatable and the PMT was translatable so that the effects of target rotation and translation on the measured speckle pattern could be compared. Standard optical chopper-synchronous detector signal processing provided good signal-to-noise (S/N) ratios even for target configurations with very small backscatter. For small angle target rotation or small receiver translation, the speckle patterns obtained from a given target were identical. Thus continuous target rotation was selected for the remainder of the measurements made during the program.

A typical speckle pattern for metallized sphere is shown in Figure 2. The effect of aperture averaging of the speckle data can be seen

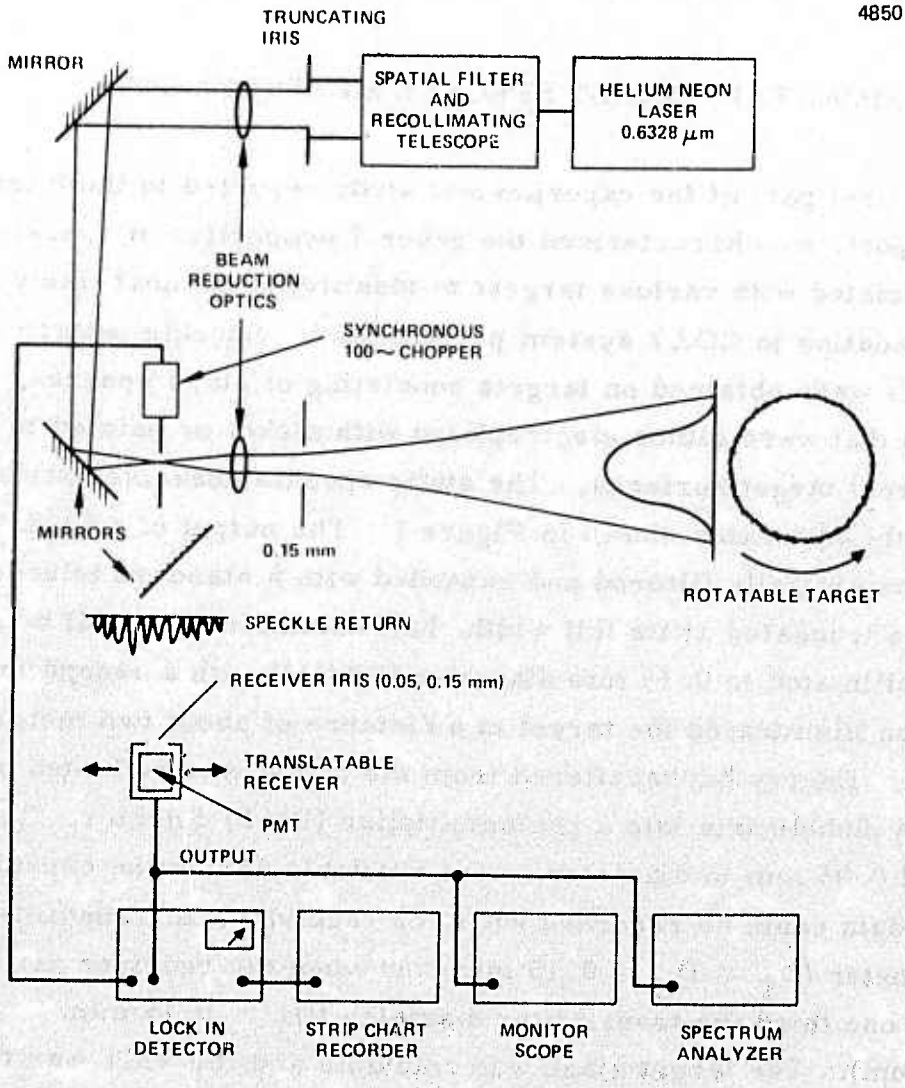

Figure 1. Measurement apparatus for study of static speckle characteristics.

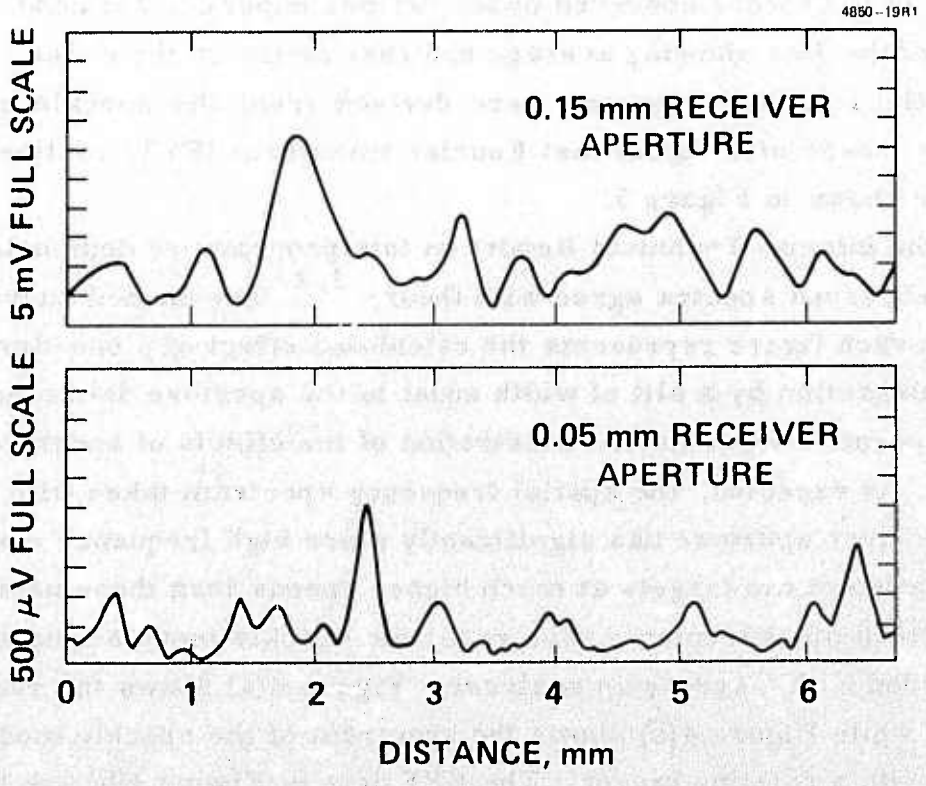

Figure 2. Speckle modulation of receiver voltage generated by rotation of a metallized sphere.

by comparing the upper trace taken with the larger aperture to the lower trace taken with the smaller aperture. The lower trace shows higher spatial frequency content. Similar speckle data were obtained from the other metallized targets studied. Maximum local contrast ratios* as high as 0.89 and as low as 0.17 were observed under various experimental conditions, with most of the data showing average contrast ratios on the order of 0.5.

Spatial frequency spectra were derived from the speckle data of Figure 2 by means of a digital fast Fourier transform (FFT) routine. These spectra are shown in Figure 3.

In the Interim Technical Report on this program we demonstrated that these observed spectra agree with theory.[1, 2] The dashed curve superimposed on each figure represents the calculated effect of a one-dimensional aperture integration by a slit of width equal to the aperture diameter. This procedure permits a qualitative illustration of the effects of aperture averaging. As expected, the spatial frequency spectrum taken with the smaller receiver aperture has significantly more high frequency content.

Rotation of the targets at much higher speeds than those used in the speckle pattern measurements gave real time speckle modulations which were recorded with a spectrum analyzer. Figure 4(a) shows the receiver noise level while Figure 4(b) shows the spectrum of the speckle modulations that occur with a rotating target. The FFT data in Figure 4(b) are found from the spatial frequency data of Figure 3 by using the relation

$$f_t = 2\Omega_T Z f_s \,, \tag{1}$$

where Z is the target range, f_t is the temporal frequency, and f_s is the spatial frequency. As can be seen, the spectrum determined by the two separate techniques are in good agreement. As discussed later, except for dither modulations, these speckle spectral data are virtually identical

---

*We define contrast ratio as $CR = (I_{max} - I_{min})/(I_{max} + I_{min})$, where I_{max} and I_{min} are the maximum and minimum observed irradiances.

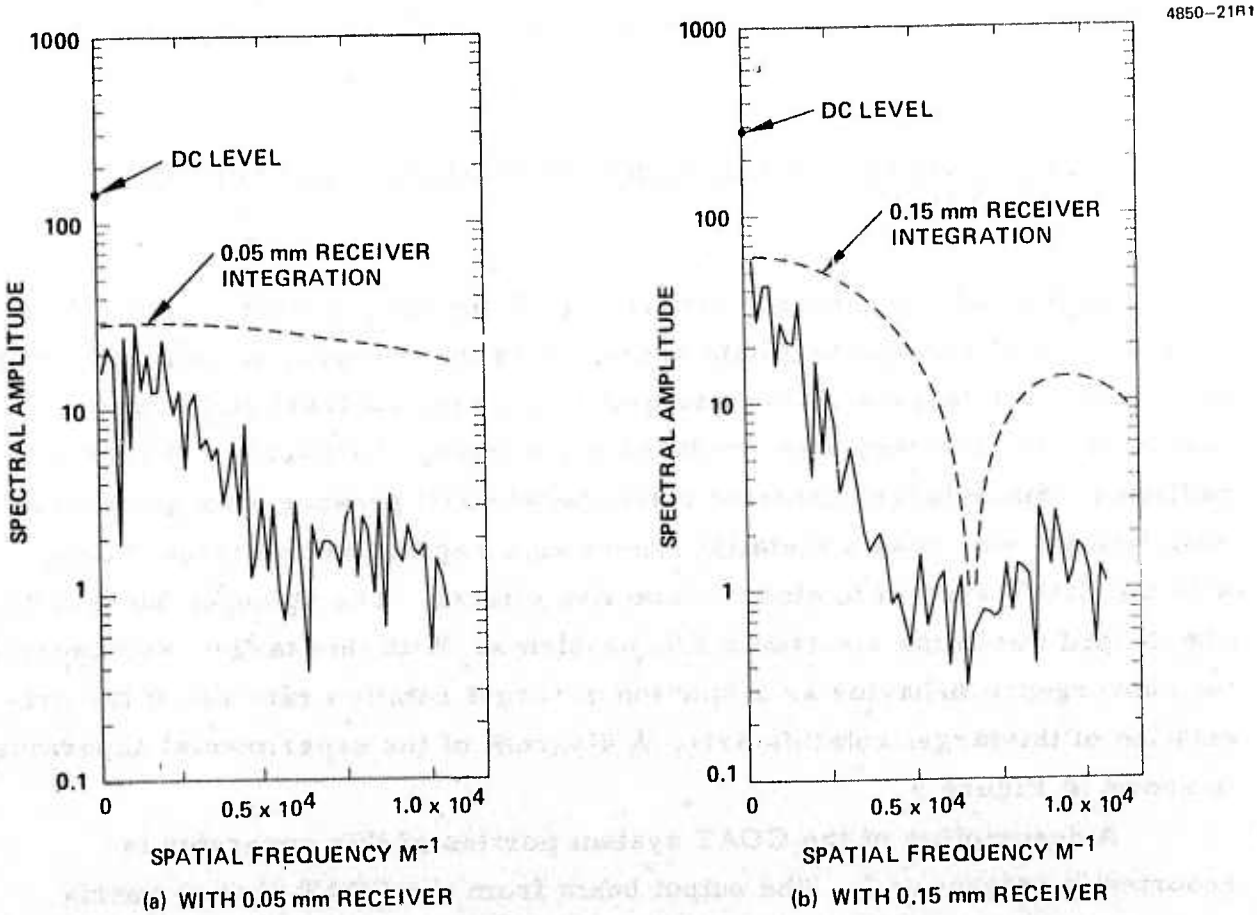

Figure 3. Spatial frequency spectra of receiver modulations generated by rotation of a metallized sphere (same as Figure 2). Dashed lines show theoretical effect of aperture averaging.

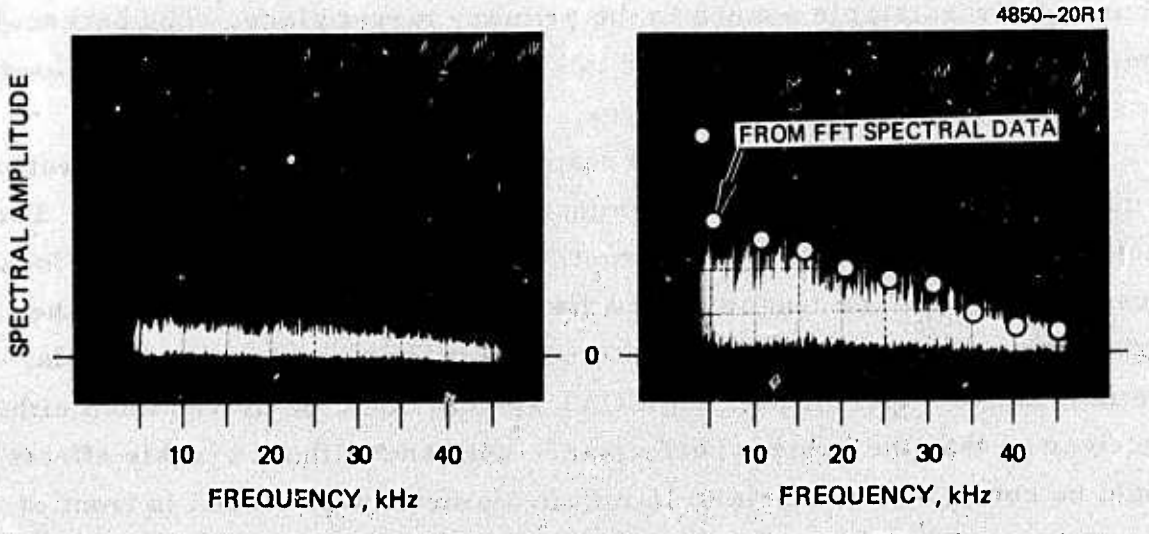

Figure 4. Speckle spectra for smooth spherical metallized target (a) Stationary target, $\Omega_T = 0$. (b) Target rotating at $\Omega_T = 0.67$ rps Spectrum analyzer bandwidth is 10 Hz.

to that obtained in later experiments when the COAT system is part of the optical source.

B. COAT SYSTEM PERFORMANCE IN PRESENCE OF SPECKLE MODULATION

In general, the speckle patterns of all the targets studied were similar. Contrast ratios and spectral data presented in the previous section were typical for metallic targets. These targets had larger contrast ratios than painted targets and they also produced more intense backscattered (180°) radiation. Since larger contrast ratio speckle will produce stronger receiver modulations, we chose a metallic sphere as a representative target to use with the COAT system to study interactive effects. The stronger backscatter also helped minimize electronic S/N problems. With this target, we observed the convergence behavior as a function of target rotation rate and of the orientation of the target rotation axis. A diagram of the experimental apparatus is shown in Figure 5.

A description of the COAT system portion of this apparatus is reported in reference 3. The output beam from the COAT phasor matrix, shown expanded in the figure, passes through a reducing telescope and a beam splitter. The primary (stronger) beam then passes through a turbulence generator and a blooming cell placed between the elements of a second demagnifying telescope. The final beam, collimated at an aperture of 0.15 mm, illuminates a rotatable sphere in the primary target plane. The backscattered energy from the target is received in PMT receiver No. 1, which is located close to the target demagnifying lens.

The weaker beam from the beamsplitter passes through an identical demagnifying telescope before illuminating a fixed secondary target. The backscattered energy from this target is received by a second PMT, located close to lens f_2. The two optical paths are thus identical except for the turbulence and blooming distortions and the tracking and focus controls. In the interactive experiments, the COAT system could be driven from either receiver so that the system performance with and without speckle effects could be compared. An iris 0.15 mm in diameter was placed in front of

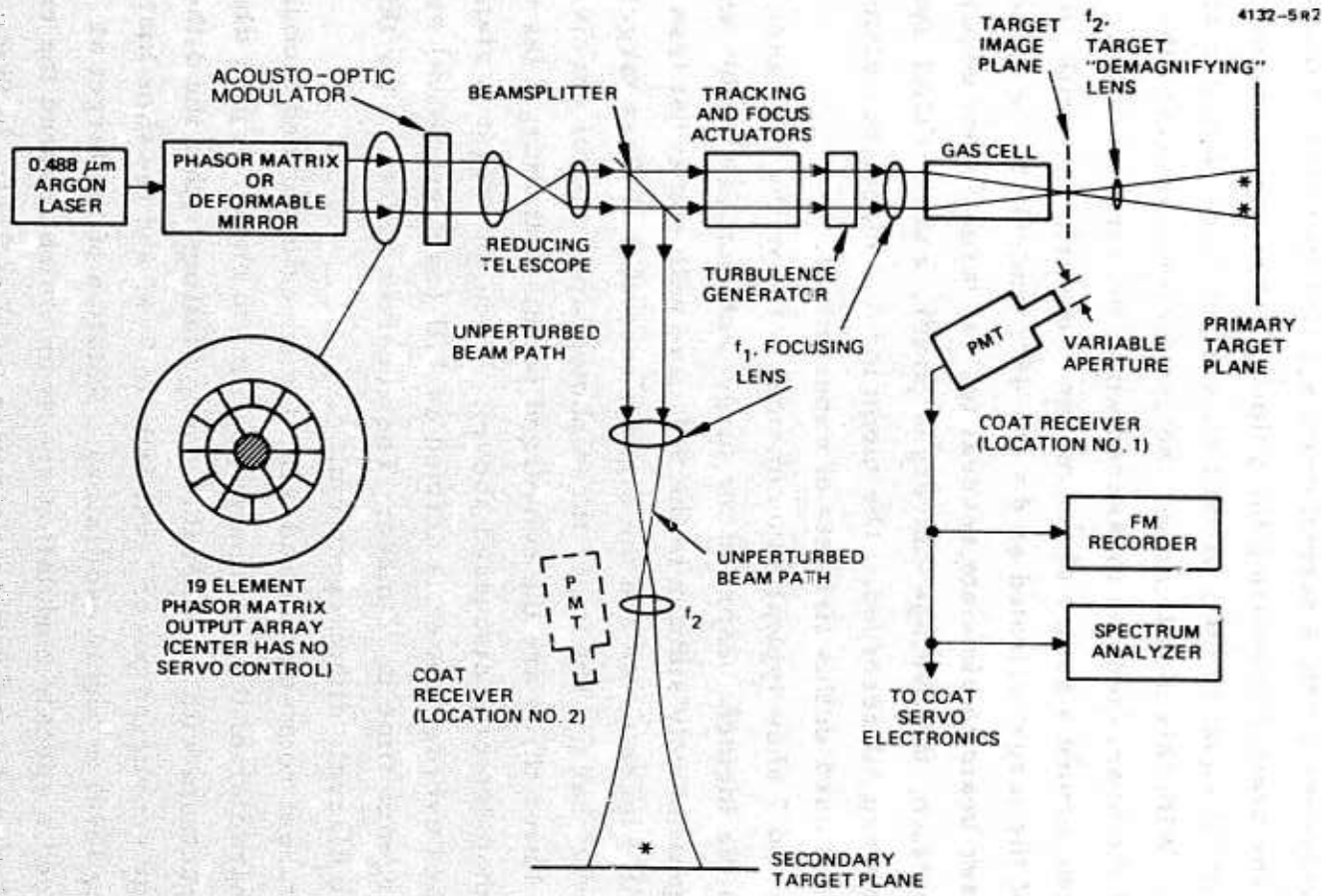

Figure 5. Block diagram of experimental arrangement used in the interactive COAT speckle experiments.

receiver No. 1 during most of our experiments to match the receiver size to the diameter of the transmitted beam. The distance from the target to both the transmitter and receiver was one meter.

Since it was not feasible to place a detector on the rotating target to measure the convergence level, a second beam splitter (not shown) was used to deflect part of the beam illuminating the primary target into a photodetector with an aperture about equal to the null-null converged beam diameter at the detector location. With this modification, the convergence time and the convergence level of the beam could be measured while the target rotated.

We first performed a series of convergence experiments with the axis of rotation of the target oriented at $\theta = 0°$, 45°, and 90° to the direction of the incident laser beam to simulate several typical target/beam encounters. The receiver spectrum, the average converged power, and the COAT system convergence time were all recorded. The blooming and turbulence distortion generators were not used in this first set of experiments.

Figures 6 and 7 show typical experimental data for the two cases when the angle between the incident beam and the target rotation axis is 90° and 0°. The 45° case is qualitatively similar to the 90° case with somewhat less degradation observed. In Figure 6, we see the signals recorded at three target rotation rates for the 90° case. The upper three photographs are the receiver spectrum and the lower three are the converged power on the target (as seen by the auxiliary photodetector discussed above). When the target is stationary, the normalized average power is defined as 1.0 (no degradation) and the system convergence time is 2 msec. The receiver spectrum for this case is simply the discrete dither spectrum.

When the target rotates at 2π rad/sec, the speckle-induced modulations cause the character of the frequency spectrum to change from a discrete to a continuous spectrum with considerable energy falling within the dither band. The average converged power level falls to 0.47 and the time history of the convergence level is highly oscillatory. Rotation of the target at 2π rad/sec produced a speckle modulation spectrum which covered the entire dither band and produced degradation to a power level of 0.31. In these measurements the gain was kept at a high level, which gave optimum convergence for static targets. The results show that significant convergence degradation can be generated by speckle modulations from moving targets

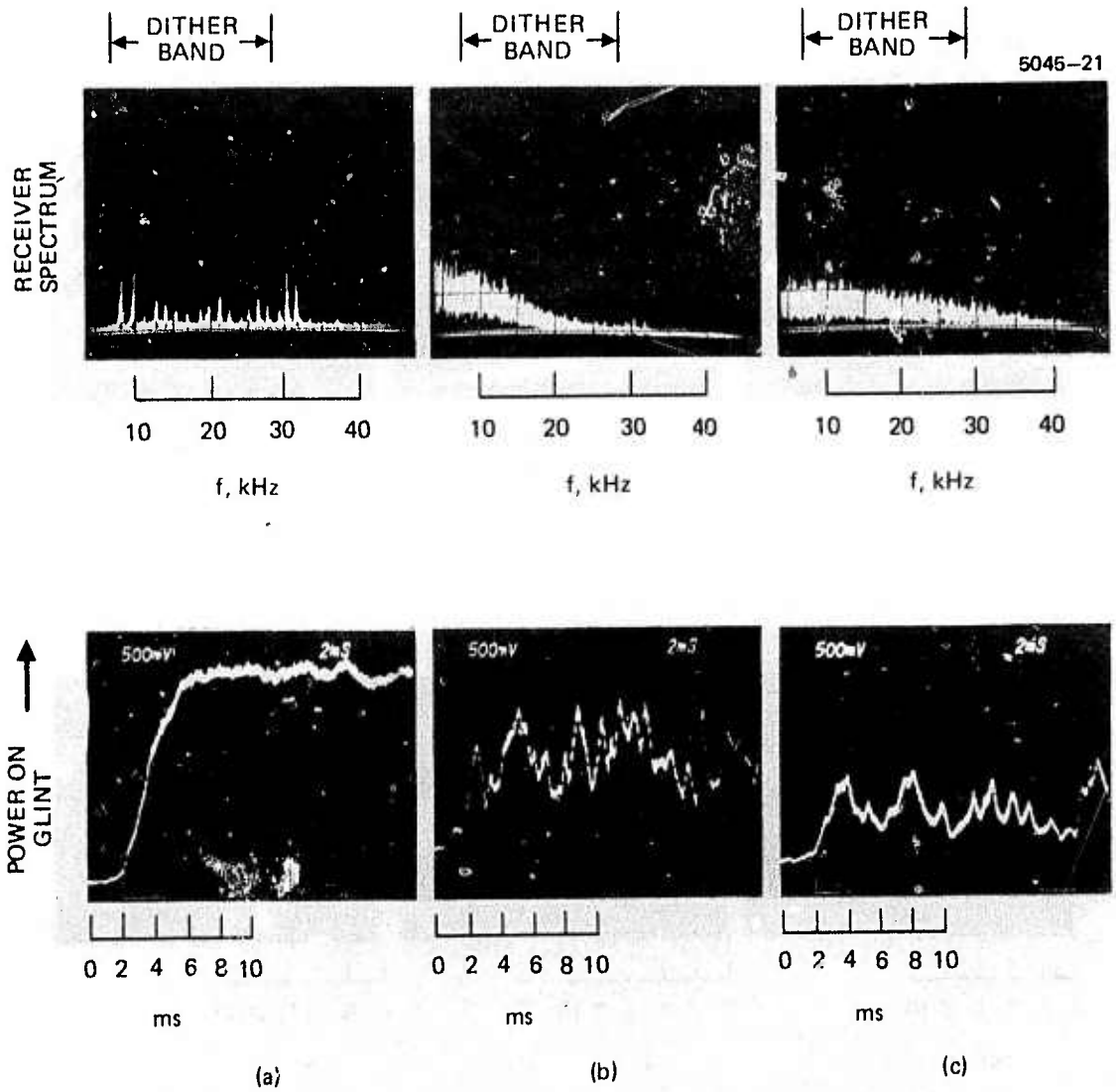

Figure 6. Experimental convergence data.

Target: Rough metal sphere, 90° orientation of rotation axis, $\lambda = 0.488\ \mu m$.

The upper pictures are outputs of a spectrum analyzer looking at the COAT receiver signal. The lower pictures show the peak target irradiance seen by a pinhole detector as the servo loop is closed.

(a) Target rotation $\Omega_T = 0$. Average power after convergence = 1.

(b) $\Omega_T = \pi$ rad/sec P = 0.70 (c) $\Omega_T = 2\pi$ rad/sec P = 0.31.

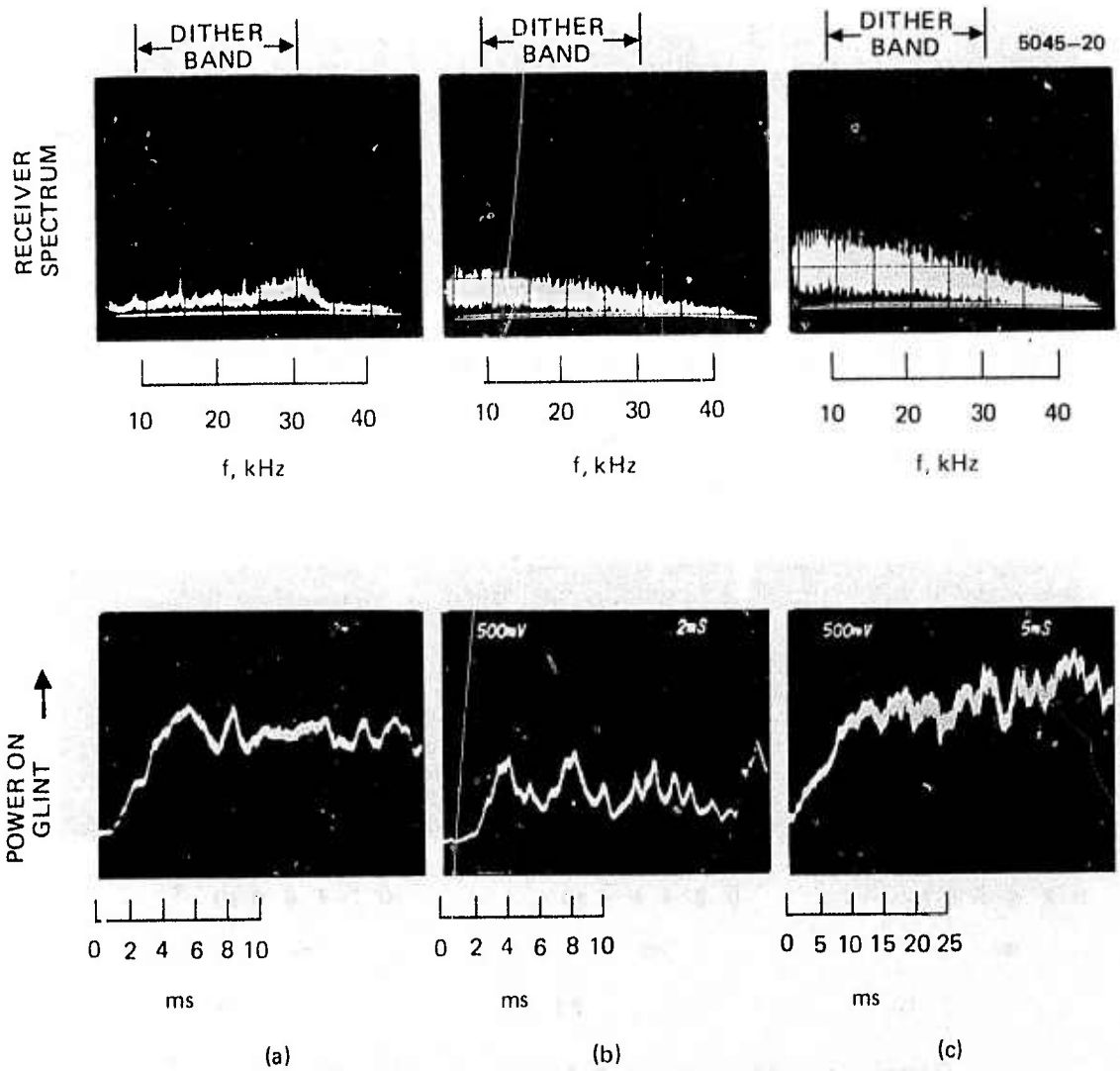

Figure 7. Effects of orientation and gain in speckle experiments. Target : Rough metal sphere, $\lambda = 0.488$ μm, target rotation rate $\Omega_T = 2\pi$ rad/sec. The upper pictures are outputs of a spectrum analyzer looking at the COAT receiver signal. The lower pictures show the peak target irradiance seen by a pinhole detector as the servo loop is closed. (a) Target orientation $\theta = 0^o$, static optimization (high gain) average power after convergence = 0.92. (b) $\theta = 90^o$ static optimization, P = 0.31. (c) $\theta = 90^o$ dynamic optimization (low gain) P = 0.93.

when the COAT system gain is optimized for a static target. If the gain is reduced, the degradation is less severe because the servo bandwidth in each channel is reduced. Thus the overall convergence level increases because less speckle modulation is passed by the servo system synchronous detectors. We show these effects in Figures 7(b) and 7(c), with the axis of rotation at 90°, and a rotation rate of 2π rad/sec. Decreasing the static optimization gain level by -15 dB produces a dynamic convergence optimization in which the mean convergence level is 0.93, compared with 0.31 for the high-gain case.

In Figure 7(a), with the target rotation axis oriented parallel to the beam (i.e., 0°), we observe very little convergence degradation. Here we see for high gain (static optimization) only minimal convergence degradation to a level of 0.92 at a target rotation speed of 2π rad/sec.

Figures 8 and 9 summarize the observed convergence levels and convergence times for all the interactive experiments. Referring to the 0° orientation case in Figure 8(a), the system performance was first optimized* with the target stationary; the convergence level was then recorded as a function of rotation rate. For this case, optimization of the system with the target rotating produced the same results. The small variations in converged power level for different rotation rates are due to glint tracking by the COAT system, which caused the converged beam to partially miss the detector aperture. Visual observation of the converged beam profile on a television monitor showed almost no degradation.

With the rotation axis at 90 degrees (Figure 8(b)), the largest degradation occurs with high loop gain (static optimization) and the smallest degradation occurs with low loop gain (dynamic optimization). The intermediate or 45° orientation case in Figure 8(c) shows speckle convergence degradation to a level of 0.45 with static optimization and recovery to a level of 0.80 with dynamic optimization. The average convergence level for all three orientations under static and dynamic optimization conditions is shown in Figure 8(d).

---

*Minimum convergence time and maximum convergence target irradiance achieved by adjusting servo loop gain.

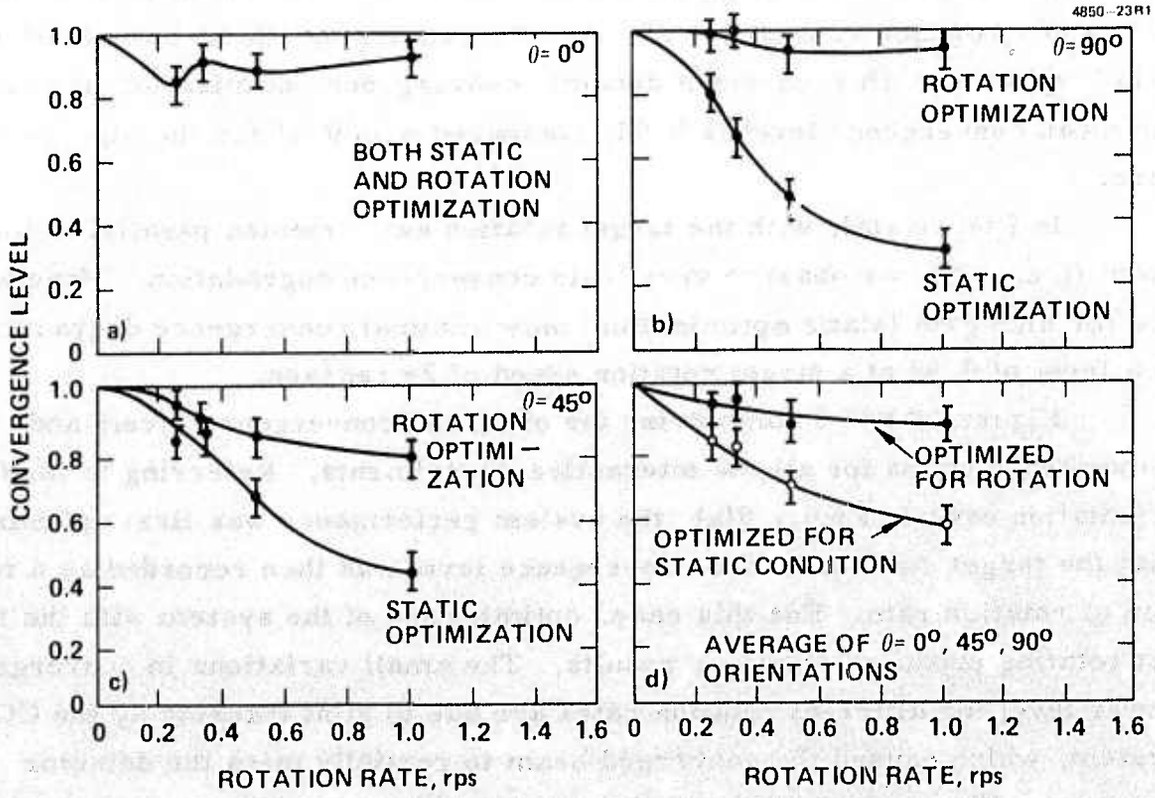

Figure 8. Summary of observed convergence levels in the presence of speckle effects. (a) Angle between t rget rotation axis and incident beam, $\theta = 0^{o}$. ( ) $\theta = 90^{o}$. (c) $\theta = 45^{o}$. (d) Data of (a), (b), and (c) averaged.

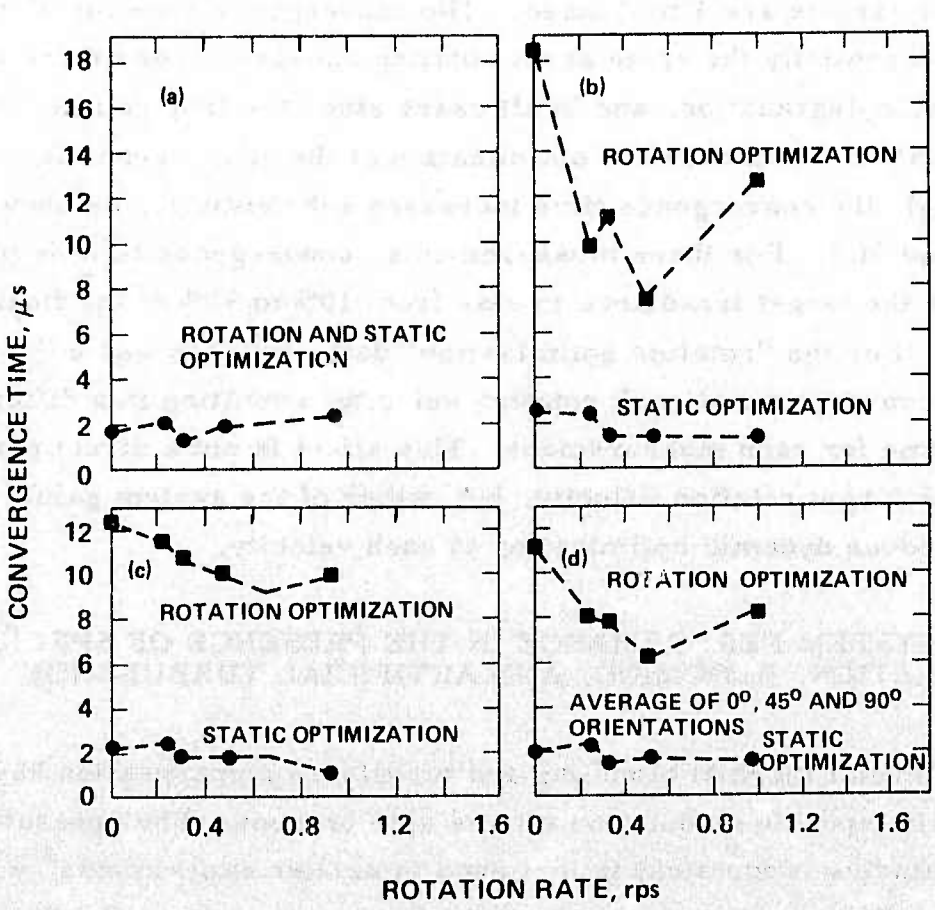

Figure 9. Summary of convergence times in the presence of speckle modulations (θ = orientation of rotation axis relative to incident laser beam). (a) $\theta = 0^{o}$, (b) $\theta = 90^{o}$, (c) $\theta = 45^{o}$, (d) average of (a), (b), and (c).

In addition to improving the overall convergence level, another effect of reducing the COAT system loop gain is to increase convergence time. The observed convergence times are shown in Figure 9. Typical convergence times for static targets are 1 to 2 msec. The convergence time for 0° target orientation is essentially the same at all rotation speeds because there was little convergence degradation, and in all cases since the loop gain is set to its maximum value. With dynamic optimization of the convergence level (or lower loop gain), the convergence time increases substantially, as shown in Figures 9(b) and 9(c). For these measurements, convergence time is defined as the time for the target irradiance to rise from 10% to 90% of the final average level. For the "rotation optimization" data, the gain was adjusted for maximum convergence at each rotation velocity, resulting in a different convergence time for each measurement. This effect is not a direct consequence of the target rotation velocity, but rather of the system gain required to produce dynamic optimization at each velocity.

C. COAT SYSTEM PERFORMANCE IN THE PRESENCE OF SPECKLE MODULATION, BLOOMING, AND ARTIFICIAL TURBULENCE

Experimental thermal blooming and turbulence compensation have been studied with speckle modulation effects also present. The apparatus used in these studies is identical to that used in earlier experiments[4] which had no speckle effects. Measurements were performed using a flowing liquid blooming cell, with the cell occupying the first 81% of the focused, 22 cm propagation path. This condition provides better correction than the case where the cell is in the last 81% of the propagation path.[4]

To ensure that the blooming distortions as a function of propagation distance are the same in the laboratory at 0.488 μm, the blooming strength, the total absorption, αZ, and the Fresnel number must be held constant. The absorption coefficient is α and the total propagation distance in the blooming medium is Z.

The Fresnel number, α_F, is conveniently defined by

$$\alpha_F = \frac{kD_T^2}{4Z} , \tag{2}$$

where $k = 2\pi/\lambda$ and λ is the wavelength, and D_T is the transmitter diameter.

The blooming strength is measured by the product $\alpha_L \cdot P_T$, where P_T is the laser power at the entrance to the blooming medium and α_L is defined for a gaseous medium by

$$\left(\alpha_L\right)_{gas} = \frac{\gamma_o(\gamma - 1)\, k\alpha\, Ze^{-\alpha Z}}{\pi\gamma r_o V_P} \tag{3}$$

The quantities γ_o, γ, P, and V are the molecular polarizability of the gas, the specific heat ($\gamma = C_P/C_V$), the static gas pressure, and the transverse wind velocity. For a liquid, α_L is

$$\left(\alpha_L\right)_{liquid} = \frac{2k\alpha Z\, (dn/dT)\, e^{-\alpha Z}}{\pi n_o \rho C_P V D_T} , \tag{4}$$

where the liquid density is ρ, the nominal index of refraction is n_o, and dn/dT is the change of index with temperature.

Because the net blooming cell transmission (windows plus liquid) was only 0.1, the receiver aperture had to be chosen with a diameter twice the transmitter in order to achieve an adequate S/N level. Some aperture averaging over the data in Section II-B is thus occurring. With the speckle-generating target in motion, system convergence was unstable at all but the highest power levels with a smaller receiver, the instability being produced more by the low S/N than by speckle effects. By increasing the receiver aperture to twice the transmitter size, we were able to obtain more reliable and reproducible data as discussed in the following subsections.

1. Blooming and Speckle

In this series of experiments, scaled according to Eqs. (2) and (3), we wanted to observe any possible interactions between the speckle and blooming phenomena and how such interactions might affect COAT performance. The blooming cell shown schematically in Figure 5 was filled with a methanol and iodine solution which gave a transmission factor of $\exp(-\alpha L) = 0.3$ for the liquid alone ($\alpha L = 1.2$). The cell was operated at a transverse wind velocity between 0.15 cm/sec and 0.55 cm/sec which produced significant convection-dominated thermal blooming. The transmitter diameter was 0.1 cm. The target rotation speed selected for the speckle measurements was always 2π rad/sec, the speed at which maximum convergence degradation is observed with the COAT system in the high loop gain condition (static optimization, see previous section). Observations of the convergence level were made at various laser powers with and without speckle effects, with and without active COAT phase compensation; and at both the high and low servo loop gain settings. The results of these experiments are shown in Figure 10.

In the absence of speckle, the COAT system improves the peak target irradiance by a factor of 2.3 and increases the critical transmitter power* by roughly the same factor. The improvements in the target irradiance at the corrected critical power ($P_T \approx 3.5$) is roughly a factor of 3.1.

In the presence of speckle effects, with the system optimized for best correction in the absence of speckle (high gain), rotation of the target at 2π rad/sec produces a converged irradiance degradation of 0.52 of the maximum at the critical power. Reduction of the servo loop gain by about 10 to 15 dB raises the converged irradiance back to a level of 0.81 of maximum. This is qualitatively similar to what we observed in the nonblooming experiments. Without the blooming, however, we observed a more severe speckle degradation and a better recovery, from 0.31 to 0.93 of the free-space, no-speckle maximum.

---

*Transmitter power at which the target irradiance is maximum when blooming effects are present.

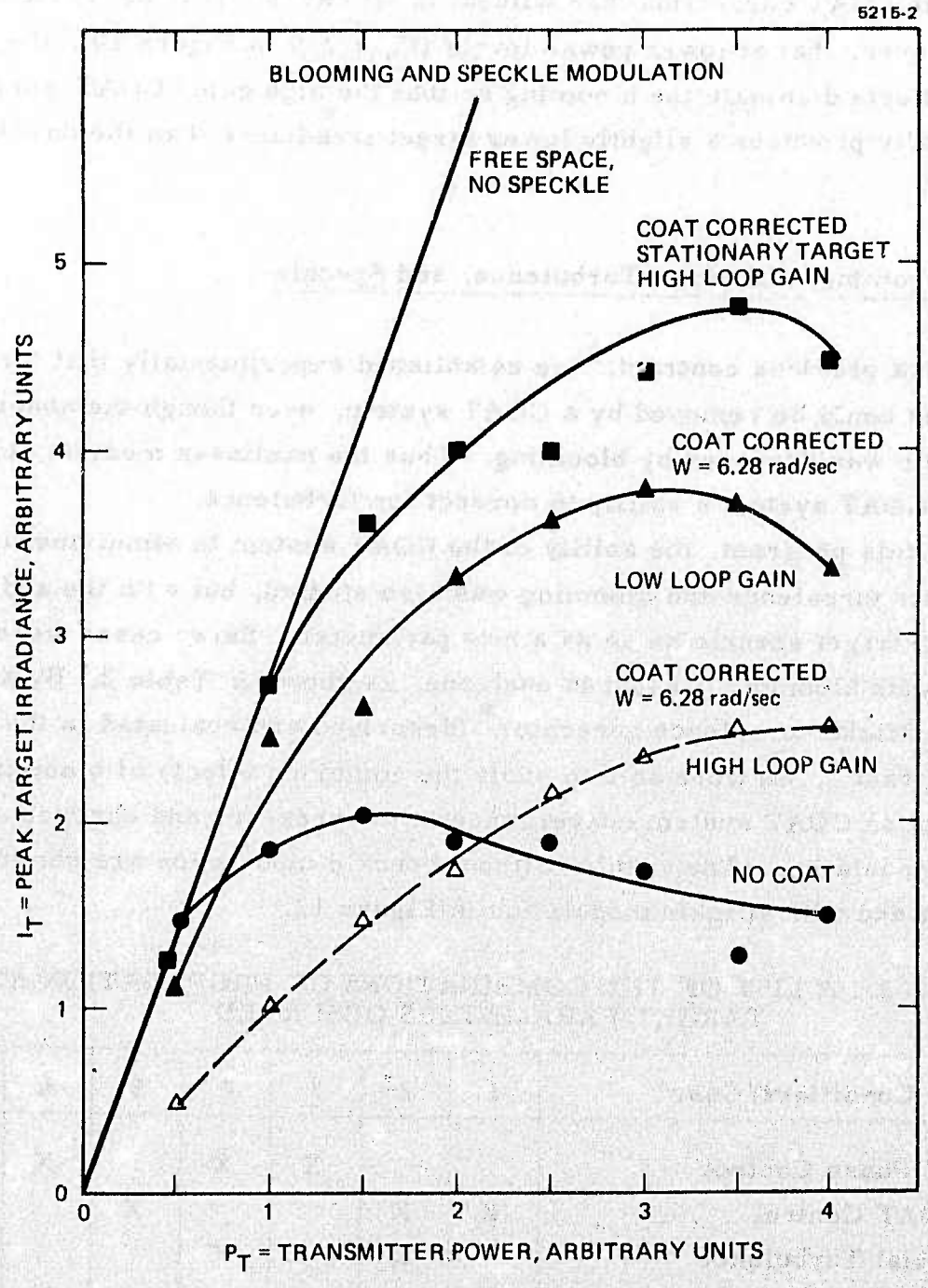

Figure 10. Target (focal-plane) irradiance with blooming and speckle, with and without COAT correction.

Nevertheless, at high power levels, the converged irradiance is higher with COAT correction than without in all cases. It is interesting to note, however, that at lower power levels ($P_T \leq 2.0$ in Figure 10), the speckle effects dominate the blooming so that the high gain, COAT-corrected case actually produces a slightly lower target irradiance than the no-COAT case.

2. Blooming, Artificial Turbulence, and Speckle

On a previous contract,[4] we established experimentally that turbulence distortions could be removed by a COAT system, even though the absolute Strehl ratio was degraded by blooming. Thus the nonlinear medium did not limit the COAT system's ability to correct for turbulence.

In this program, the ability of the COAT system to simultaneously compensate turbulence and blooming was also studied, but with the addition of moving-target speckle noise as a new parameter. Seven cases were studied, with blooming present in each one, as shown in Table 2. By activating the artificial turbulence generator* (described and evaluated in the previous contract[4]), we were able to study the combined effects of blooming and turbulence on COAT system convergence in the presence and absence of speckle modulation. The results without speckle modulation are shown in Figure 11 and with speckle modulation in Figure 12.

TABLE 2. A LIST OF THE COMBINATIONS OF PROPAGATION AND TARGET PARAMETERS OBSERVED

Conditions/Case	1	2	3	4	5	6	7
COAT Phase Control			X	X		X	X
No COAT Control	X	X			X		
Artificial Turbulence		X		X			X
No Turbulence	X		X		X	X	
Target Rotation at 2π rad/sec					X	X	X
No Speckle Modulation	X	X	X	X			

*A single phase screen moving close to the transmitter aperture.

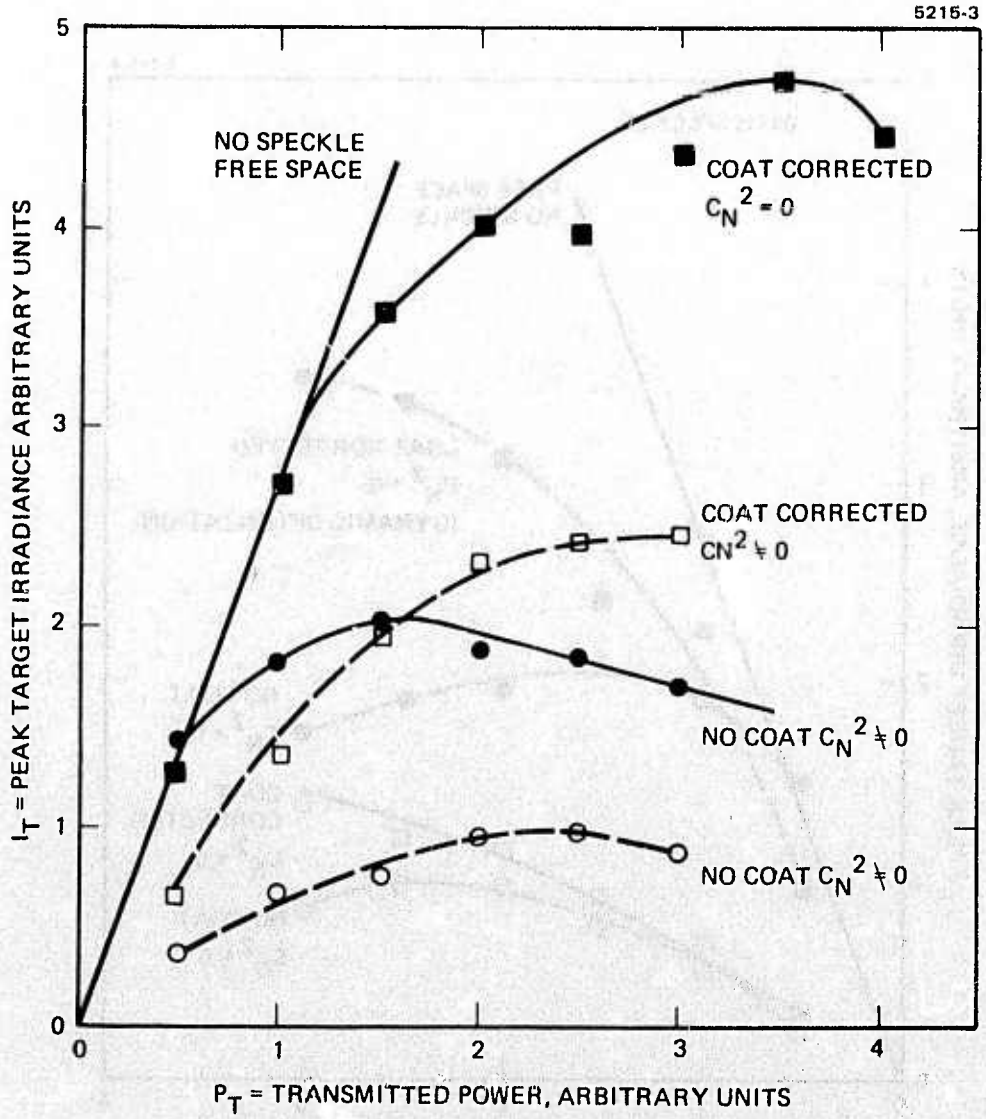

Figure 11. COAT convergence with blooming and turbulence, but with no speckle modulation effects (stationary target). The $C_N^2 = 0$ curves are the same as in Figure 10.

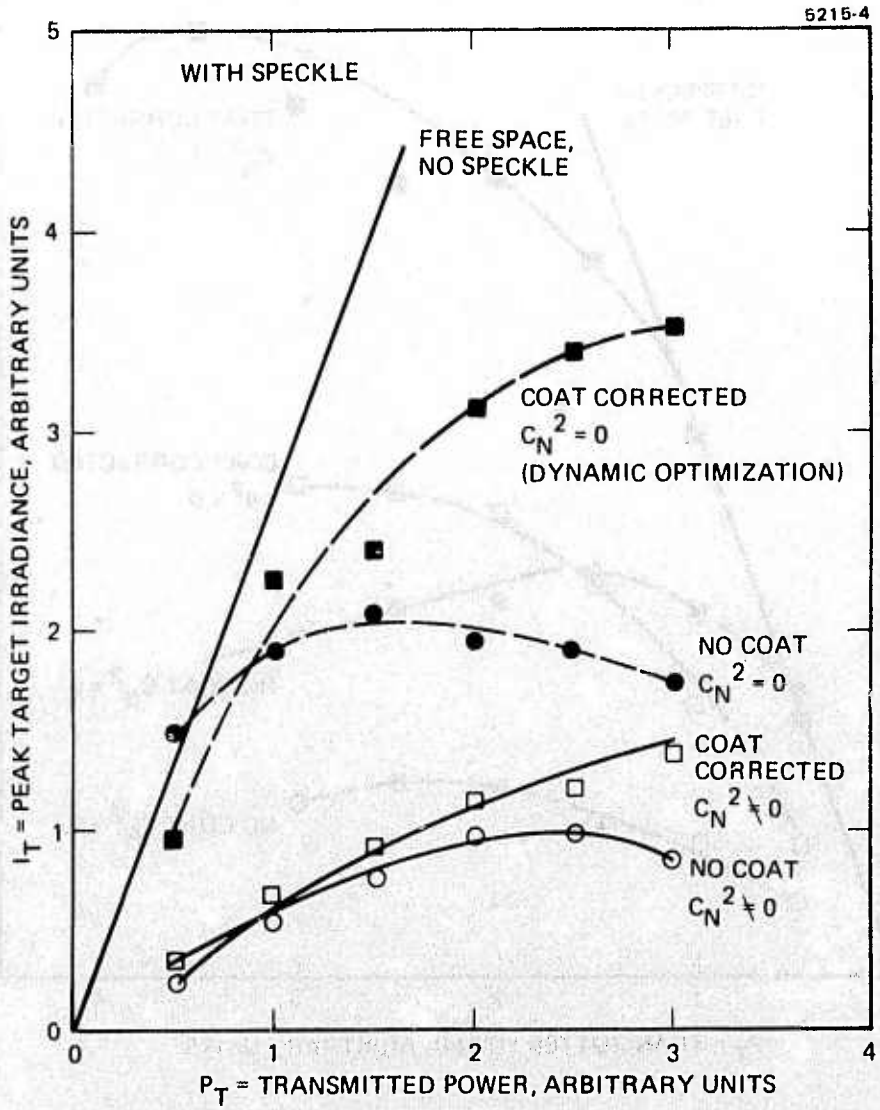

Figure 12. COAT convergence with blooming, artificial turbulence, and speckle modulation effects. Target rotation rate, Ω_T = 6.3 rad/sec.

There are several things to note about the data in Figure 11. First, the COAT system cannot fully correct for the turbulence; the strength of the turbulence is too great for the finite number of phase correction elements. The effect is seen at low transmitter power where the slope of the "COAT corrected, $C_N^2 \neq 0$" curve falls below the free space line and the "NO COAT, $C_N^2 = 0$" line. Significant turbulence compensation is occurring, however, since the "COAT corrected, $C_N^2 \neq 0$" curve falls well above the "NO COAT, $C_N^2 \neq 0$" curve. Second, in the presence of blooming and turbulence, the COAT system produces about a factor of 2.5 increase in peak target irradiance. In fact, at all power levels more than a factor of 2 correction is observed. Finally, we conclude, as we have previously,[4] that the turbulence compensation capacity of a multidither COAT system is not significantly affected by the presence of blooming distortions.

When speckle effects are added to these experiments, a reduction in peak target irradiance occurs for the COAT-corrected cases, as expected. The results are shown in Figure 12. All of the COAT-corrected data in Figure 12 were taken with a lowered servo loop gain ("dynamic optimization" as used earlier). Very little turbulence compensation is observed; the convergence degradation caused by speckle, about a factor of 2, is just enough to offset the improvement in Figure 11 resulting from turbulence compensation, also about a factor of 2.

Note, however, that blooming compensation is only slightly affected by speckle as seen earlier in Figure 10. With no turbulence ($C_N^2 = 0$), the peak irradiance is increased by COAT correction about a factor of 1.7, which is less than the factor of 2.3 in Figure 11, but still significant. The lack of turbulence compensation observed with these severe speckle effects is not well understood since significant blooming compensation occurs, indicating that the COAT system phase correction capabilities are not completely lost. As a possible explanation, we hypothesize that the speckle degrades the high frequency error correction capability of the COAT servo more than the low-frequency correction. In effect, the effective servo error correction bandwidth has been reduced. The very low electronic S/N ratios present in our experiments may also contribute to the poor turbulence compensation with speckle. That is, when the S/N is low, any noise-like disturbances (such as

speckle) have more effect on the system and the high frequency servo error correction capability is reduced. We have observed similar poor turbulence correction behavior in other experiments where there were no speckle effects, but which had very poor electronic S/N. At this writing, however, we have no way to uniquely isolate electronic S/N effects from purely speckle-induced effects for the data in Figure 12. The data definitely indicate that the turbulence compensation capability of a COAT system is strongly affected by speckle, and that the blooming correction is also reduced, but much less so.

SECTION III

ANALYTICAL AND COMPUTER SIMULATION TECHNICAL ACCOMPLISHMENTS

A. THEORETICAL ANALYSIS OF MULTIDITHER COAT SERVO RESPONSE TO SPECKLE MODULATION

A comprehensive analysis has been developed during the course of this program to explain the convergence behavior of COAT systems in the presence of spurious modulations due to speckle. These results have been partially reported in Interim Report No. 1 of this contract.[5] An updated documentation of these results is given in the Appendix of this report and summarized here very briefly.

The analysis predicts average convergence levels as a function of the average power in the spurious electrical signal in the COAT servo due to speckle-induced intensity modulations at the receiver. In order to predict the convergence level, we must assume that the average power spectrum of the modulations is known or can be determined. Since the power spectrum is a function of the degree of convergence of the incident beam, of target surface characteristics, and of target motion, all this information must be known. The analysis neglects the change in power spectrum with convergence level. Nevertheless, in order to be conservative we have assumed a target illumination near full convergence since this will give speckle lobes on the order of a transmitter diameter. Lower convergence levels will result in smaller speckles which can be more easily averaged by the receiver aperture. We are thus considering only power spectrums which are worst cases in virtually all physical applications. Knowing the power spectrum and the COAT servo bandwidth allows us to calculate the average power in the spurious electronic signals. Using a statistical model of the convergence process, we then calculate the average power in the true error signal in the COAT servo at the various dither frequencies. The average convergence level is then determined

based on the assumption that the power ratio, ρ', of the dither signal to the speckle-induced signal after demodulation is unity. Computer simulation studies discussed in the next section have validated this assumption.

In a typical multidither COAT system, the servo bandwidth in a given channel is a function of the gain in that channel. The gain, on the other hand, depends on the overall convergence level and the error in that channel. The average power in the speckle signal will therefore also vary as a function of convergence level due to this variation in bandwidth. This effect can be included in the analysis by calculating an average bandwidth for all the channels as a function of convergence level. This would involve another independent analysis of the COAT servo and because of limited time was not done as part of this study. In lieu of a complete first-principles calculation, we have verified the analysis by comparing its predictions to computer simulations using an artificial modulation function whose power spectrum consisted of very narrow bands around each dither frequency. The bands were chosen narrow enough so that they would always be narrower than the servo bandwidth. Thus, there could be no variation in the spurious modulation power due to changes in the convergence level. The results, which show excellent agreement between analysis and computer simulation, are shown in Figure 7 of the Appendix. If the analysis of the bandwidth variations is completed as part of future programs, we expect to be able to show similar agreement between analysis and computer simulation for any realistic power spectrum.

The principal result of this analysis is that we can now analytically predict the average convergence level of a COAT system if two parameters are well specified: power spectrum of the speckle modulations and COAT servo bandwidth. If these variables can be specified as a function of convergence level, then iterative calculations can be made which will predict the correct level. If they cannot be specified as a function of convergence level, then less accurate but conservative predictions can still be made. Another important result of the analysis is that comparison with computer simulations indicate that the maximum fluctuations about the average convergence level are also predictable. The computer simulations (as well as the experimental observations discussed in the previous chapter) showed that the convergence level in the presence of speckle effects oscillates randomly

between two levels. The analysis indicates that the maximum level is reached when the power in the speckle signal is twice the power in the dither, that is when $\rho' = 0.5$, and the minimum level occurs when $\rho' = 2.0$.

B. COMPUTER SIMULATION RESULTS

During the first phase of this contract, computer simulations were run using a set of three realistic speckle modulation data generated by the General Research Corporation (GRC).[6] The physical scenario consisted of a rotating target sphere (1 m radius) uniformly illuminated with 10.6 μm coherent radiation over a 10 cm diameter spot at a range of 2 km from the COAT receiver. This illumination function corresponds roughly to a diffraction-limited spot from a 25 cm diameter transmitter. The data itself consisted of time histories of the intensity variations at the receiver for three target rotation rates, $\Omega = 0.01$, 2, and 10 rad/sec, with the rotation axis oriented perpendicular to the illuminating beam direction. These results along with some of our reservations about the data were reported in the last interim report.

Since the previous report, we have resolved our questions about their model and a new set of data was supplied by GRC. This data included aperture averaging over an annular receiver surrounding a transmitter with an outside diameter of 1.2 m and an inner diameter of 1.0 m. A new calculation technique using statistical methods to calculate the intensity variations or modulation functions was also employed. This technique overcomes the problem encountered in the earlier data where the modulations were periodic with a period of approximately 0.5 msec caused by a finite number of sample points in a point target model. The new data again consisted of three modulation functions representing the same physical scenarios, except that the slowest target rotation rate was $\Omega = 0.4$ rather than 0.01 rad/sec. A schematic diagram of the scenario is shown in Figure 13.

We found that all three of these modulation functions produced noticeable degradation in COAT performance. The amount of degradation depends on both the speckle modulation itself and on the choice of servo parameters. The principal observable effects are (1) a decrease in the

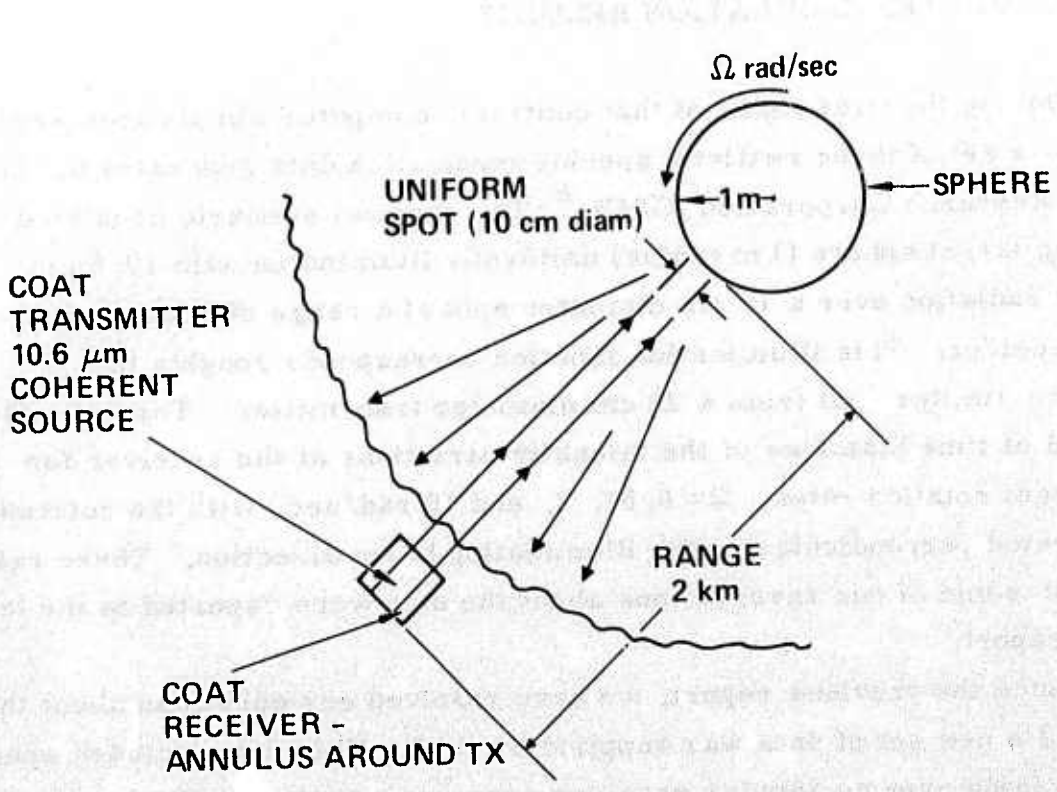

Figure 13. Physical scenario used to calculate a realistic speckle modulation function.

mean convergence level, and (2) random oscillation of the mean level at frequencies on the order of 0.5 to 1.0 kHz. Of the various servo variables, the open loop gain G_1 and the signal amplitude limiter (clipper, see Figure 14) had the most noticeable influence in reducing these effects. Both the experiments and the computer simulations demonstrate that reducing G_1 from its optimum value for performance without speckle will increase the degraded mean convergence level when speckle modulations are present. This has the undesirable effect of also increasing the convergence time (decreasing the servo control bandwidth). Signal amplitude limiting can also produce an increase in the mean convergence level for selected values of the amplitude limit and for certain ranges in the value of G_1. The effect on convergence time, on the other hand, is much less noticeable.

In order to pick the best values of these parameters, an optimization study was conducted using the realistic speckle modulation function with the target rotating at 2.0 rad/sec, chosen because it produced the most severe degradation in COAT performance. Figures 15 and 16 summarize the data gathered during this study. Figure 15 shows that for each clipping level there is an optimum gain where the convergence time is minimum. Increasing or decreasing the gain from this level causes slower convergence. In Figure 16, for the same set of clipping levels, we see that the highest mean convergence levels occur at lower gains than those associated with the smallest convergence times. The bars in this figure represent the extremes of the oscillatory variation in the convergence level referred to earlier. The value of signal clipping is demonstrated by comparing Figure 16(a) and 16(d). In Figure 16(d) the low clipping greatly reduces the oscillations in the convergence level and improves the mean convergence level, except at very low gains. In Figure 15(d), however, we see that this value of clipping level tends to increase the convergence time. In the optimization study, these tradeoffs were considered, and we chose $G_1 = 1000$ and a clipping level of ± 0.3 as a reasonable compromise for both high convergence level and fast convergence time. All three of the GRC scenarios were then simulated using these values of clipping and gain.

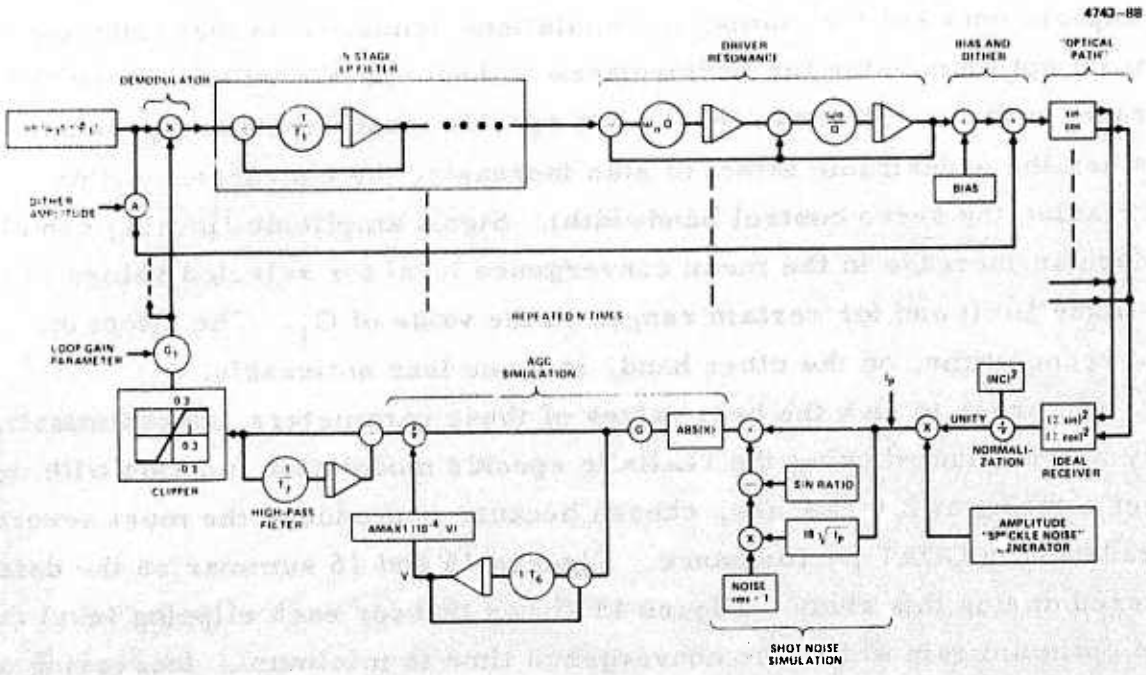

Figure 14. Schematic diagram of multidither servo simulation.

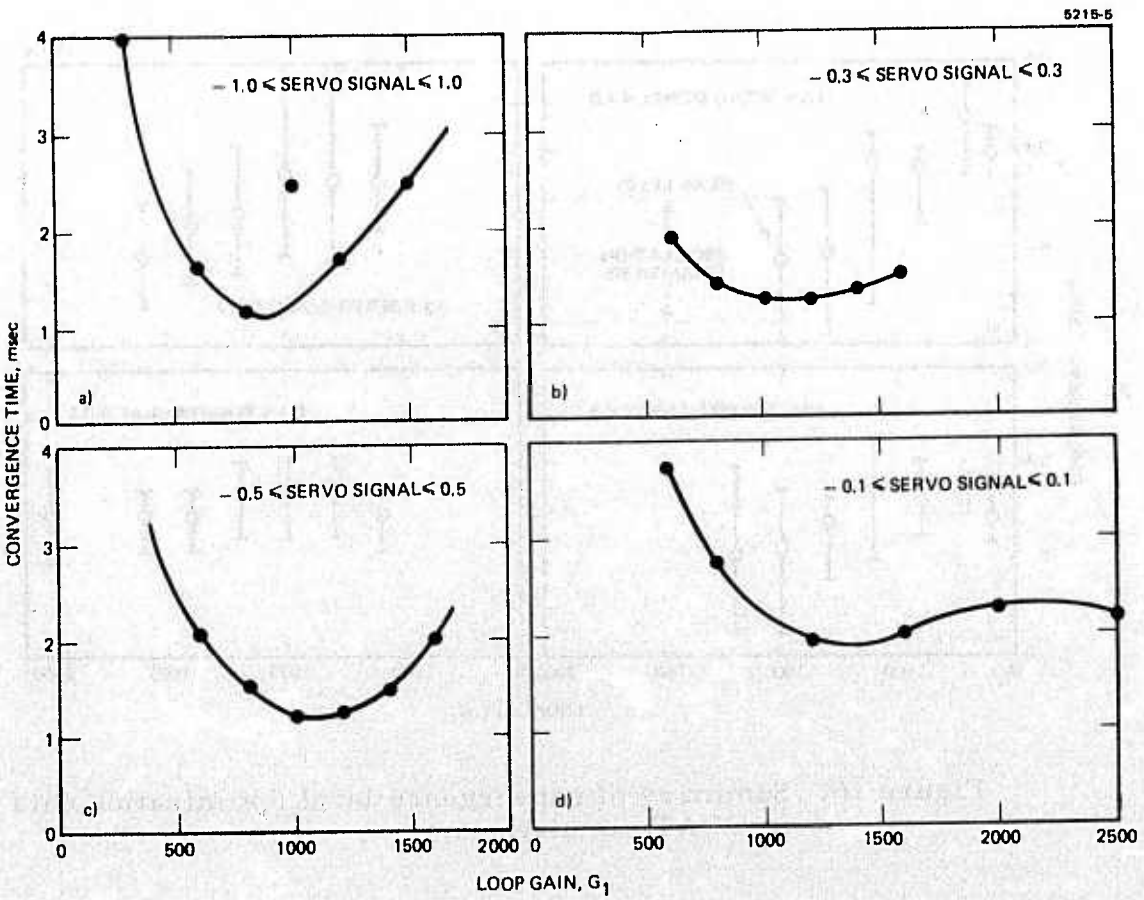

Figure 15. Summary of convergence time optlmization data in COAT simulations.

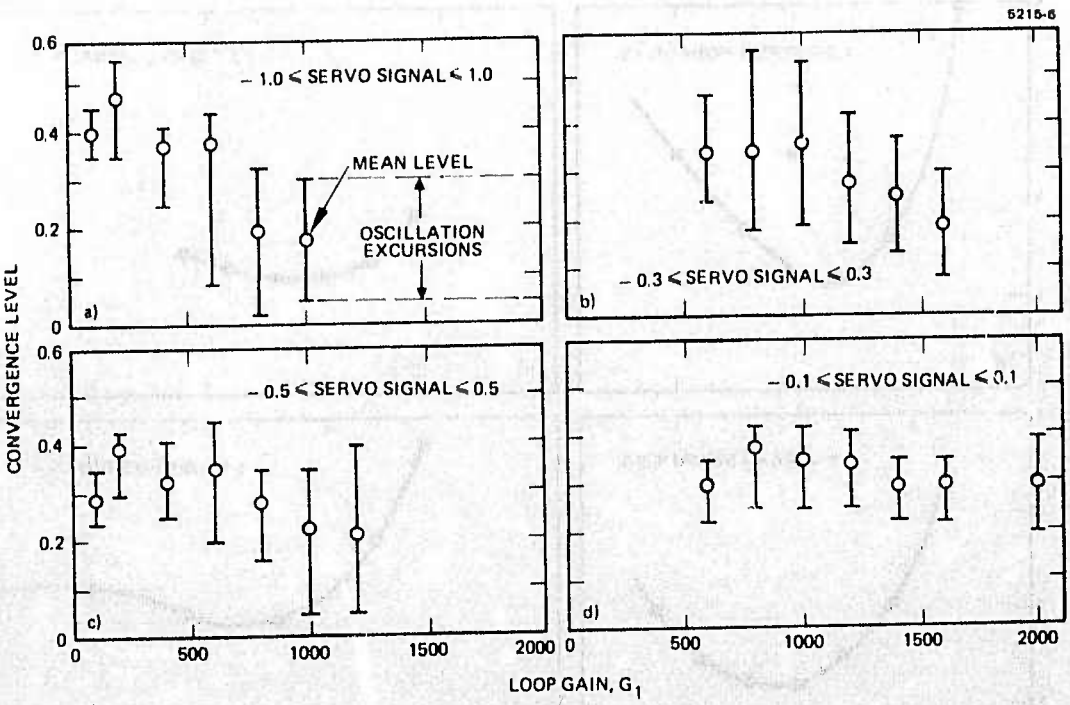

Figure 16. Summary of convergence level optimization data in COAT simulations.

Figures 17, 18, and 19 show the three GRC modulation functions, their Fourier spectrum, and the resulting COAT performance in the form of a time history of the intensity on a target glint normalized to unity at full convergence. (The two time histories superimposed on each other correspond to COAT performance with and without speckle modulations for easy comparison.)

The most obvious conclusion from these simulations is that the modulation power in the dither band is the overriding speckle parameter which will affect COAT performance. At a slow rotation rate (Figure 17), most of the power is at the frequencies below the dither band. At the higher rotation rate of 2 rad/sec (Figure 18), much of the power spectrum falls in the dither band. At the highest rotation rate, 10 rad/sec (Figure 19), the power spectrum spreads over a large frequency range; consequently there is less power in the dither band than in Figure 19. The most severe degradation occurs for the case in Figure 18 where most of the spectral power is in the dither band. Increasing or decreasing the rotation rate redistributes the power spectrum outside the dither band with a resultant improvement in COAT performance.

These results can be compared to analytical predictions subject to the limitations described earlier. At this writing, we can only estimate what the average servo bandwidth corresponding to each simulation actually is, since the actual bandwidth is a function of time and varies from channel to channel. Our best estimate indicates that an average of ±100 Hz around each dither frequency is a reasonable number for all three simulations, for the choice of G_1 = 1000 and clipping level = ±0.3. We thus calculate the three speckle coefficients* based on this bandwidth. The results of these calculations along with the corresponding predicted convergence levels using Figure A-9 of the appendix are shown in Table 3. The observed convergence levels in the computer simulations are also shown for comparison. Note that the agreement is reasonable, with the analysis tending to be pessimistic in its prediction. With a proper calculation of an average servo bandwidth, we feel the agreement will improve.

---

*See appendix for definition of speckle coefficient, C_s.

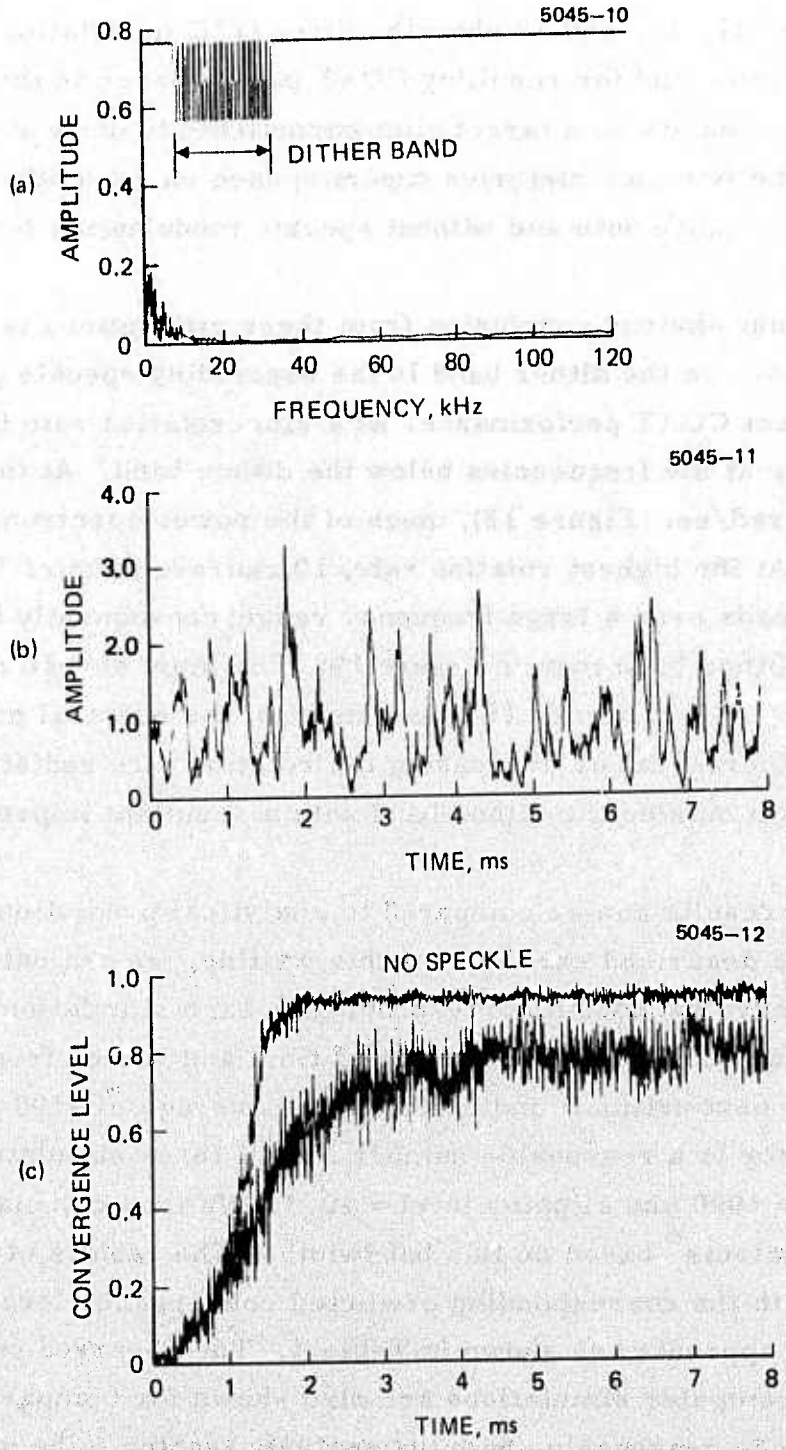

Figure 17. Summary of computer simulation results with realistic speckle modulations from a spherical target rotating at 0.4 rad/sec at a range of 2 km from receiver. (a) Fourier spectrum of speckle modulations. (b) Time history of speckle modulations. (c) Time history of COAT performance.

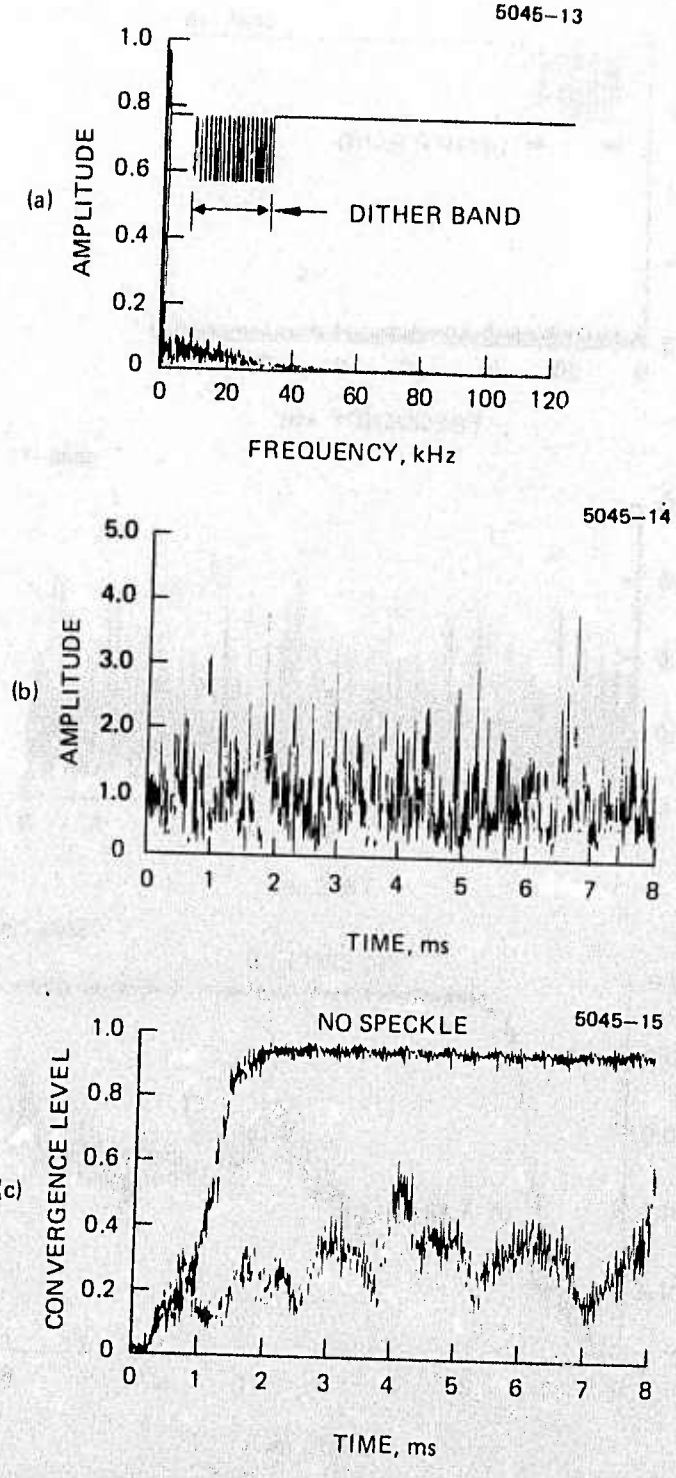

Figure 18. Summary of computer simulation results with realistic speckle modulations from a spherical target rotating at 2.0 rad/sec at a range of 2 km from receiver. (a) Fourier spectrum of speckle modulations. (b) Time history of speckle modulations. (c) Time history of COAT performance.

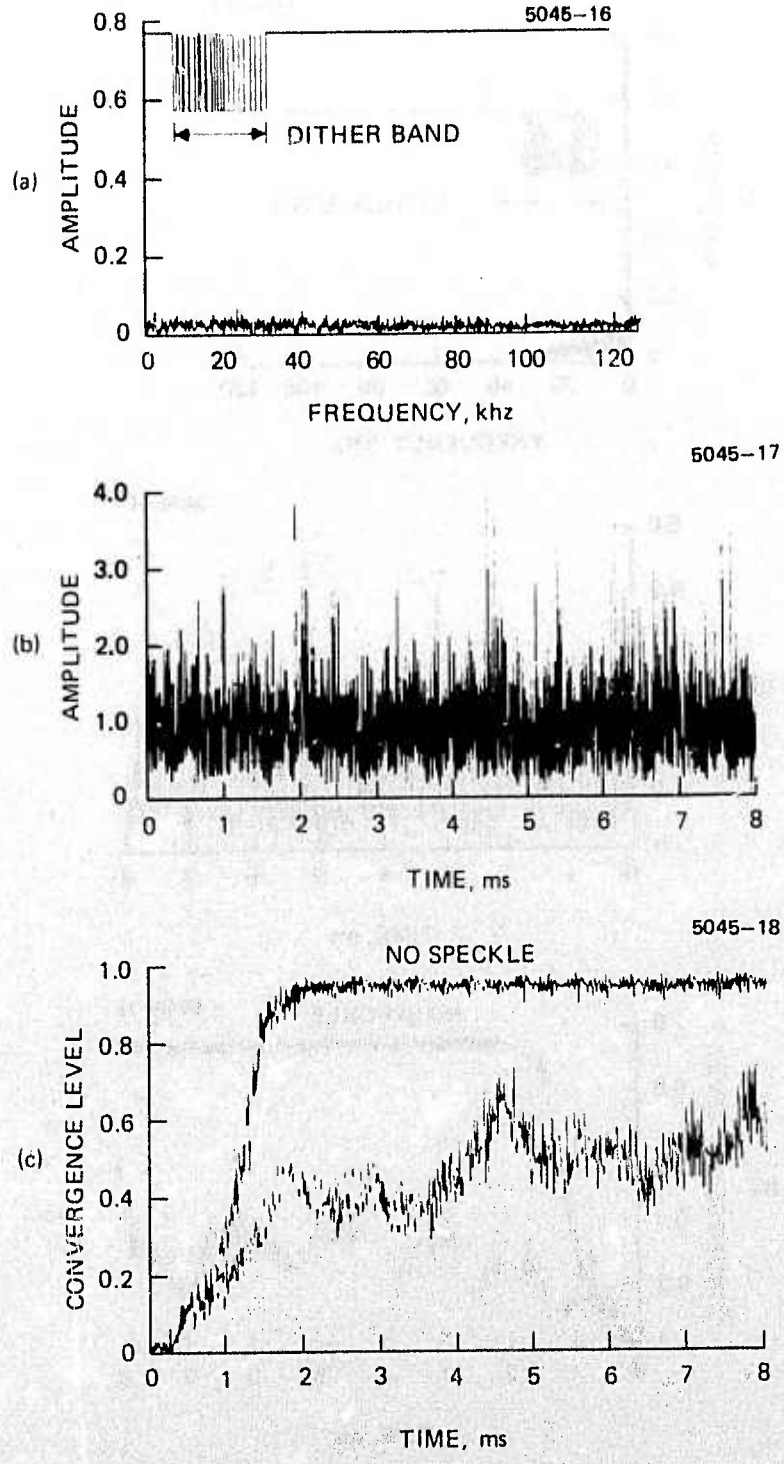

Figure 19. Summary of computer simulation results with realistic speckle modulations from a spherical target rotating at 10.0 rad/sec at a range of 2 km from receiver. (a) Fourier spectrum of speckle modulations. (b) Time history of speckle modulations. (c) Time history of COAT performance.

TABLE 3. COMPARISON OF ANALYTICAL SPECKLE MODEL WITH COMPUTER SIMULATIONS FOR REALISTIC SPECKLE MODULATIONS

Target Rotation Rate (rad/sec)	Computer Simulation Convergence Level			C_s Calculated from Simulation	Analytically Predicted Convergence Level		
	max	min	avg		max	min	avg
0	0.95	0.95	0.95	0	0.95	0.95	0.95
0.4	0.86	0.72	0.74	0.07	0.87	0.68	0.79
2	0.42	0.22	0.32	0.24	0.39	0.05	0.18
10	0.62	0.40	0.51	0.18	0.56	0.15	0.36

Other servo parameters can also be used to some degree to help improve COAT performance. Increasing the dither amplitude, ψ, for example, increases the dither signal power relative to the speckle modulation power, with a resulting increase in convergence level. Beyond a given amplitude which depends on the severity of the degradation, however, one reaches a point of diminishing return because the maximum possible convergence level decreases with increasing dither amplitude. This result is illustrated in Figure 20. The solid curve is the theoretical maximum convergence level, while the data points are from computer simulation runs using the artificial speckle modulation function of Eq. A-27, in the appendix, with the amplitudes a_{jk} chosen randomly between 0 and 0.012. This corresponds to a speckle coefficient, $C_s = 0.095$. If $\psi = 20°$ is considered the nominal dither amplitude, one can achieve some improvement in convergence level by increasing ψ to 35°, but beyond this value increasing ψ will only cause more degradation.

During this program we also found that changing to square wave demodulation in the synchronous detection process seemed to reduce the convergence level degradation caused by speckle modulations. The observed effect is shown in Figure 21. The two time histories have identical servo parameters except that part a) has square wave demodulation while part b) has sine wave demodulation. The limited time available for the study of square wave demodulation only permitted observation of this effect in a few simulations. We therefore offer no explanation as to why it should produce this apparent improvement. We only document it in this report for completeness.

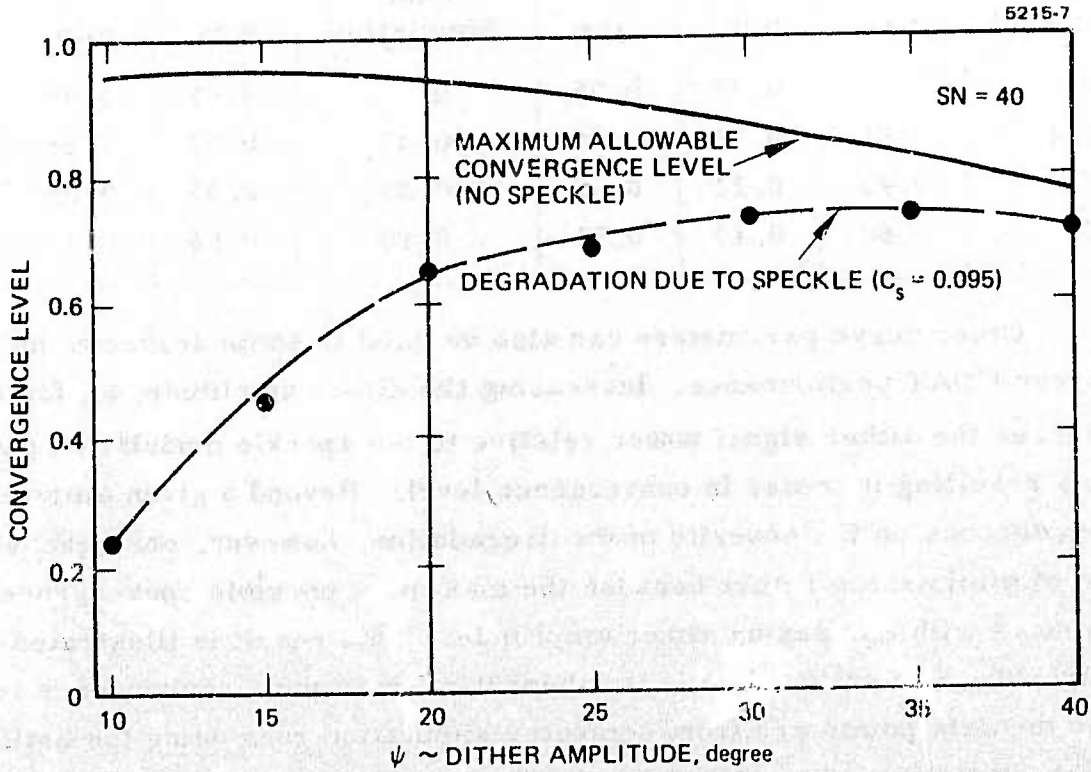

Figure 20. Effect of increasing dither ar[illegible]e on COAT convergence level degraded by [illegible]kle.

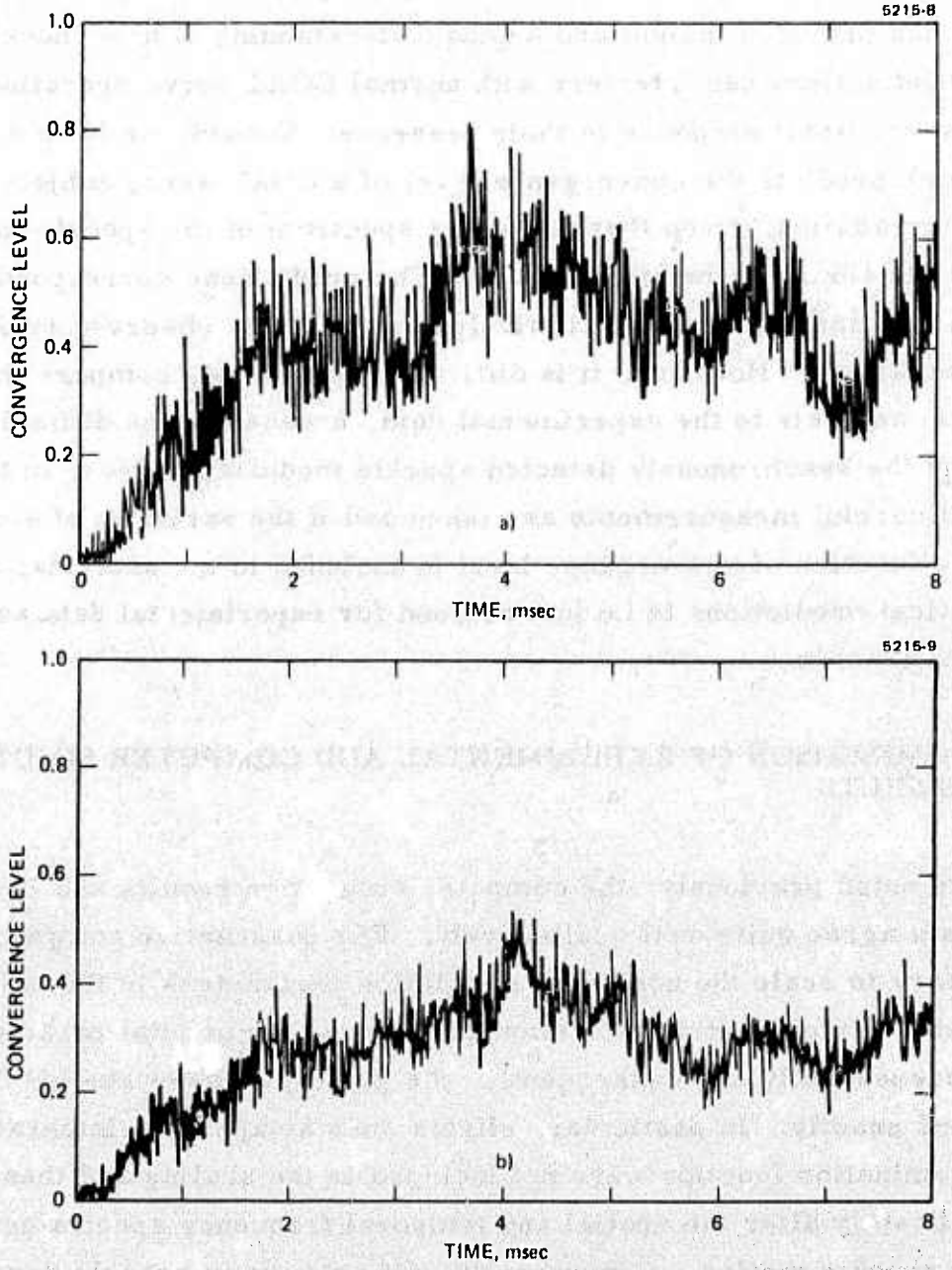

Figure 21. Observed effect of square wave synchronous detection on COAT convergence level degraded by speckle (a) square wave demodulation (b) sine-wave demodulation.

The principal accomplishments of the analytical study are twofold. First, it has provided insight and a good understanding of how speckle-induced modulations can interfere with normal COAT servo operations and how the servo itself responds in their presence. Second, we have developed a tool which predicts the convergence level of a COAT array subject to speckle degradation, given that the power spectrum of the speckle modulations and the servo bandwidth is known. The predictions correspond very well both qualitatively and quantitatively to the results observed in the computer simulations. However, it is difficult to adequately compare the theoretical analysis to the experimental data, because of the difficulty in measuring the synchronously detected speckle modulation power in the COAT servo. If careful measurements are taken and if the variation of servo bandwidth as a function of convergence level is included in the analysis, we expect the analytical predictions to be just as good for experimental data as they are for simulation data.

C. COMPARISON OF EXPERIMENTAL AND COMPUTER SIMULATION RESULTS

As noted previously, the computer simulation results and the experimental data agree quite well qualitatively. For quantitative comparison, it is necessary to scale the computer simulation parameters to the laboratory experiment. Unfortunately, the simulation and experimental parameters were chosen independently and consequently, the principal cases studied do not correspond exactly. In particular, effects such as aperture integration and target illumination function were not included in the scaling and these effects can significantly alter the spatial and temporal frequency spectra generated by target speckle motion. Consequently, differences in speckle degradation of convergence will be observed.

In spite of these limitations, it is still useful to compare two cases whose Fourier power spectrum are very similar. Throughout this report we have stressed that speckle-induced power in the dither band is the crucial parameter in determining COAT performance. We will now demonstrate that computer simulations and experimental data both agree quantitatively as well as qualitatively when we compare cases subjected to the same speckle

power spectrum. For a rigorous comparison of the rotating sphere scenarios used in the experiments and simulations, one should first scale the diameter of transmitter, receiver, and illuminated target spot size to have the same ratios; second, we should require the contrast ratios to be the same; and third, the spatial frequency distributions should be proportional. With all the above requirements met, we would then scale the target range and rotation rate using the relationship

$$\frac{\Omega_T Z}{D_T} = \text{constant} , \tag{5}$$

where Ω_T is the target rotation rate, Z is the target range, and D_T is the transmitter diameter. This insures that the temporal frequency distribution is the same. Since the analytical model used at GRC for the speckle modulation calculations assumed random spatial phase distribution for the reflected target radiation, and since the laboratory targets where optically very rough, the resultant contrast ratio of both speckle patterns is probably the same in any two experimental and simulation cases we wish to compare. The case that comes closest in other comparable parameters are the 2 rad/sec simulation case of Figure 18 and the 2π rad/sec experimental case of Figure 6. Table 4 lists the parameters used in each case. There are a number of differences between the actual experiment and an exact scaling. First, the simulation assumes a uniform illumination across a 10 cm diameter spot at the target. Inferring a transmitter diameter from this gives D_T = 25 cm, which is considerably smaller than the 1.2 m x 1.0m annulus used for the receiver. A fair amount of receiver averaging is therefore occurring in the computer simulation. On the other hand, if a 2.5 cm diameter uniform spot, corresponding to a diffraction limited 1.0m transmitter, were used to illuminate the target, the rotation rate would have to increase by about a factor of 4, to 8 rad/sec, to produce about the same power within the COAT system dither band. The experimental illumination function is roughly Gaussian.*

*Actually closer to $J_o^2(r)$, but the distinction is not important.

TABLE 4. EXPERIMENTAL AND COMPUTER SIMULATION PARAMETERS FOR MOST CLOSELY CORRESPONDING CASE

Parameter	Simulation	Experiment
λ, wavelength	10.6 μm	0.488 μm
Z, range	2 km	1m
D_T, Transmitter aperture diameter	≈25 dm (inferred from uniform illumination of 10 cm spot at target)	0.15 mm
D_R, Receiver aperture	1.2m x 1.0m annulus	0.15 mm, filled aperture
Ω_T = Target Rotation Rate	2 rad/sec	2π rad/sec
Target Surface	Completely diffuse (randomizes reflected phase front)	Completely diffuse

The uniformly illuminated target gives rise to a linear dependence of speckle spectral density on spatial frequency whereas the Gaussian-illuminated target produces a Gaussian dependence. The receiver aperture integration or weighting function for the circular experimental aperture and the annular simulation aperture also differ.

The point to be made here is that since the various parameters do not correspond exactly, it is likely that the target rotation rate required to produce a given effect experimentally will differ from that given by the scaling rules. In fact, this was the case. Using the scaling rules in Eq. (5) directly gives 3 rad/sec for the experimental rotation rate that should give speckle effects corresponding to the 2 rad/sec simulation case. This rotation is roughly a factor of 2 lower than the 2π rad/sec rate used. Nevertheless, when one compares the two power spectra (see Figure 6 and 18), which is really the crucial consideration, we see they are almost identical, and consequently the resulting convergence levels are also almost identical. The 10.6 μm scenario computer simulation shows an average convergence level of 0.32 with oscillations between 0.22 and 0.42. The experimental observation in Figure 6 has a mean of 0.31 with oscillations roughly between 0.18 and 0.55. An additional observation that lends credence to the comparison

is that in both cases, increasing the rotation rate did not cause any more degradation in convergence level. This indicates that both power spectra correspond to rotation rates that produce maximum degradation in COAT convergence levels.

We have also performed a series of experiments to observe the effect of receiver size. In these experiments, the ratio of receiver to transmitter diameter was varied and the normalized convergence levels were recorded with the target rotating at 2π rad/sec. Table 5 shows the results of these experiments. Beginning with equal transmitter and receiver apertures, doubling of the receiver aperture raises the convergence level from 0.30 to 0.50 (a factor of 1.66). Referring to Figure A-7 in the Appendix, we see that C_s decreases by a factor of 0.74 for this change in convergence level. Since the speckle noise power is proportional to the product of the square of C_s and the convergence level (see Eq. A-27 in Appendix), we can infer a reduction of the speckle signal power by a factor of 0.66 when the receiver diameter is doubled. Thus aperture integration does indeed help to overcome speckle effects.

TABLE 5 EFFECTS OF RECEIVER APERTURE SIZE

D_R/D_T	Convergence Level
1	0.30
2	0.50
3	1.0

SECTION IV

CONCLUSIONS AND SUGGESTIONS FOR FUTURE WORK

The purpose of these investigations was to develop an understanding of the interactive effects of a multidither COAT servo with the spurious modulations induced by speckle. We have demonstrated experimentally and verified theoretically that speckle modulation generated by the motion of ordinary target surfaces can under some conditions degrade the convergence behavior or corrective ability of a COAT system. Factors such as the ratio of receiver size to transmitter size, target velocity or rotation rate, and COAT system feedback loop gain and clipping level all influence the susceptibility of the COAT system to speckle.

Some of the sensitivity to scenario and COAT system parameters is shown in the following examples: (1) Under speckle modulation conditions where the COAT system is severely degraded to a level of 0.3 of the maximum convergence level, doubling the receiver diameter increases the convergence level to 0.5; (2) Under the condition of high feedback loop gain, increasing the target rotation rate increases the degradation until a maximum is reached. Increasing the rotation rate beyond this point leads to less degradation. There thus exists a rather narrow "window" of target motions that produce significant problems; (3) With maximum speckle degradation, reducing the COAT servo loop gain by 10 to 15 dB usually removes most of the convergence degradation but with an increase in convergence time and decrease in correction bandwidth; Judicious application of clipping in the servo loop in the presence of speckle modulation diminishes the convergence degradation with little change in convergence time; and (4) Square wave demodulation and larger dither amplitude can also improve performance.

Thus the degree to which the COAT system is affected by speckle is very dependent on the COAT system parameters as well as the target parameters. The crucial speckle parameter C_S, represents the combined speckle power within the servo bandwidth around each dither frequency. The worst case computer simulation results obtained correspond to $C_S = 0.24$ and an average convergence level of 0.32. A factor of 2 reduction in speckle

contrast ratio by itself would reduce C_S to 0.12 and lead to a significant increase in average convergence level (to 0.6). In our target signature characterizations, we found a factor of 2 variation between the speckle contrast ratio of a metallized sphere and a painted sphere, and a factor of 4 variation in the contrast ratio of a metallized sphere compared to a side-illuminated metallized cone. Laser bandwidth and the ratio of target roughness to optical wavelength also offset the contrast ratio strongly. Another significant point of interest is that there was effectively no speckle modulation effect for the nose-on-target case, where the axis of rotation coincides with the laser propagation direction. This is the most probable encounter aspect in many scenarios. Because of these effects, it is not unreasonable to expect less than the theoretical worst-case speckle degradation in a real target situation.

Another system consideration is that the speckle degradation is determined by the ratio of dither power to speckle power. By increasing the dither power, we can reduce the effect of speckle. The process is limited, however, because convergence is also degraded by the very large dither amplitudes. When other system factors such as clipping level and loop gain are optimally adjusted for a specific situation, the convergence degradation due to speckle modulation can also be reduced independently of target effects. Another possible system technique for reducing the effects of speckle is optimal predictive filtering[7] (Kalman filtering).

As a final comment on how system parameters can affect speckle properties, we consider what happens when the laser illuminating the target is not monochromatic, as is the case for high-power HF/DF (3.8 μm) and CO (5 μM) lasers. To examine the effect of several laser lines illuminating the target simultaneously, it is necessary to know the ratio of the rms surface roughness, $\bar{h}$, to the optical wavelength, λ. As shown below, target surfaces with rms roughnesses on the order of 0.1 wave or less can be considered totally specular and the speckle problem can be ignored. For rougher surfaces, the intensity of the speckles and their spatial frequency spectrum will have to be calculated.

Under certain circumstances, the presence of multiple laser lines can be very beneficial in reducing the effects of speckle. For rough surfaces, each laser line generates a partially uncorrelated speckle pattern and when

the multiline speckles are combined the effect is to wash out the (single-line) speckle pattern in the same way that completely incoherent radiation washes out speckle. The following first-order analysis illustrates qualitatively what might be expected for an HF/DF or CO laser.

Consider a reflecting surface with rms roughness $\bar{h}$ illuminated by monochromatic light of wavelength λ. It can be shown that the correlation coefficient for the separate speckle patterns from two monochromatic sources with a small wavelength difference $\Delta\lambda$ is

$$\xi = \exp\left[-\left(\frac{4\pi}{\lambda^2}\,\Delta\lambda\bar{h}\right)^2\right] \quad . \tag{6}$$

By defining $\xi = e^{-1}$ as a decorrelation criteria, the wavelength decorrelation dependence is found to be

$$\frac{(\Delta\lambda)_d}{\lambda} = \frac{\lambda}{4\pi\bar{h}} \quad . \tag{7}$$

We see that the decorrelation wavelength difference is inversely proportional to the surface roughness. Figure 22 shows a plot of minimum change in wavelength needed to decorrelate a speckle pattern as a function of surface roughness calculated using Eq. (7).

A typical HF/DF laser will oscillate simultaneously on many lines. The exact lines and their relative strengths depend on many factors, including the resonator coupling fraction, but typical values for the maximum and minimum frequency spacings between lines are on the order of 0.34 μm to 0.17 μm, respectively. This gives $\Delta\lambda/\lambda$ values of 0.09 to 0.0033, respectively. Referring to Fig. 22, we see that some of the widely spaced adjacent lasing lines become uncorrelated for reflecting surfaces with rms roughness on the order of 1.0 wavelength and that as the surface gets rougher, more of the lines become uncorrelated; finally at roughness on the order of 10 wavelengths, all the adjacent lines speckle patterns become uncorrelated.

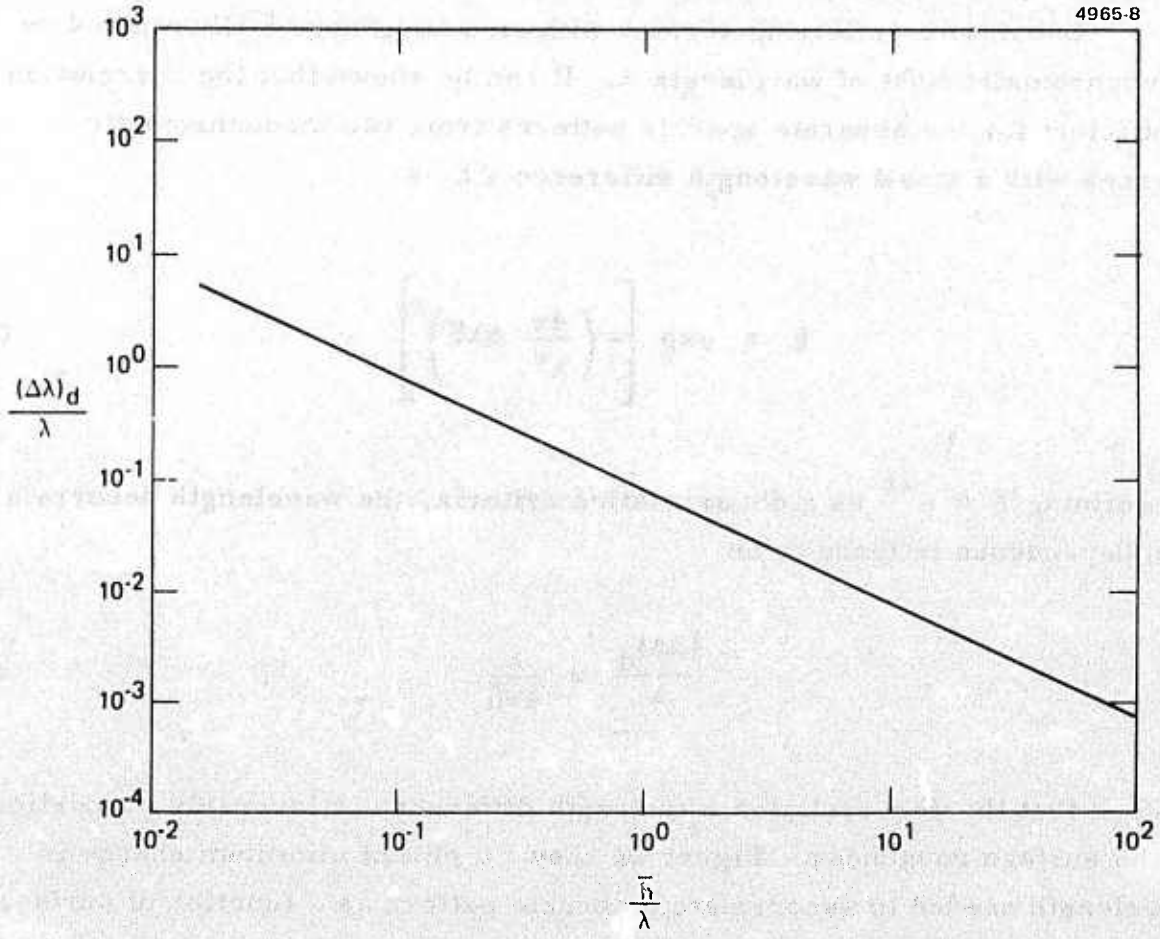

Figure 22. Decorrelation wavelength versus roughness.

For typical CO lasers, , values for $\Delta\lambda/\lambda$ range from 0.002 to 0.085. From Figure 22, an rms surface roughness of $\bar{h}/\lambda \approx 50$ is required to decorrelate the closely spaced lines, but a roughness of $\bar{h}/\lambda \approx 1.0$ is required for the largest line-pair spacing.

We thus can see that the nature of the target surface as well as the illuminating laser bandwidth play important roles in determining the severity of speckle modulation effects.

In the presence of blooming the convergence degradation due to speckle modulation was approximately the same as in the absence of blooming (once the effect of a larger receiver is accounted for in our experiments). When the effects of blooming, speckle, and artificial turbulence were simultaneously present, the COAT signal-to-noise ratio was marginal at all but the highest input power levels. At those levels, we found that the COAT system produced an improvement of 65% in peak target irradiance over the uncorrected beam. However, the degradation due to speckle in the presence of blooming and turbulence was 42%, compared to approximately 70% observed in the earlier experiments. This is accounted for by the receiver aperture being twice as large as before, and by the fact that the system was operating with poor signal-to-noise ratio and was not strongly converged in the absence of speckle. In conclusion, the effects of speckle modulation with and without the presence of blooming and turbulence are qualitatively and quantitatively the same.

Additional work is warranted to define those scenarios that can produce significant speckle modulations for high-power COAT system designs and to assess the probability of occurrence for such scenarios. The ability of advanced techniques to remove or reduce speckle effects should be explored for those scenarios where a significant problem exists. Among the items not addressed quantitatively by this contract are the effects of modulation index (particularly automatic control), number of channels, location of dither frequencies, and of allowing the speckle itself to change as the COAT convergence level changes. Inclusion of the variation of servo bandwidth with convergence level would increase the usefulness of the analysis.

REFERENCES

1. L.I. Goldfischer, J. Opt. Soc. Am. 55, 247 (1965).

2. N. George, unpublished.

3. J.E. Pearson, W.B. Bridges, S. Hansen, T.A. Nussmeier, and M.E. Pedinoff, Appl. Opt. 15, 611 (1976).

4. J.E. Pearson, S.A. Kokorowski, and M.E. Pedinoff, "COAT Measurements and Analysis," Final Report on Contract F30602-75-C-0001, RADC-TR-76-55, (A023479).

5. M.E. Pedinoff, S.A. Kokorowski, and J.E. Pearson, "COAT/Target-Signature Interactions," Interim Report on Contract F30602-76-C-0021, RADC-TR-76-64, (A026258).

6. G. Gurski, J. Radley, and J. Wilson, unpublished.

7. R.F. Ogrodnik, J. Opt. Soc. Am. 65, 1213 (1975).

APPENDIX A

THEORETICAL ANALYSIS OF COAT SERVO RESPONSE TO SPECKLE MODULATION

A. MODEL OF SPECKLE EFFECTS ON A COAT SERVO

The effect of speckle on a multidither COAT servo can be simply understood by considering the diagram in Figure A-1. The intensity of the coherent radiation, I_R, reflected off a target glint is averaged over a COAT receiver aperture. The electrical signal, S, from the receiver to the COAT servo is directly proportional to I_R and, in the absence of speckle, I_R is directly proportional to I_T, the intensity at the glint:

$$S \equiv K I_T, \text{ (no speckle)} \quad , \tag{A-1}$$

where K is the proportionality constant. The signal, S, thus varies instantaneously (neglecting the short propagation time) with any change in I_T. In general the overall effect of speckle is to spatially modulate the intensity at a given plane. The spatial modulation results from the interference of light reflected from surface irregularities on the target. Temporal modulation of the intensity at a point results from target motion which in turn causes the speckle pattern to move. The photodetector signal S is thus amplitude modulated at rates that depend on the speckle lobe size and the receiver geometry and with a modulation depth that depends on both the speckle contrast ratio and the receiver geometry. We represent this modulation by a function $M_s(t)$ which multiplies the signal S:

$$S = KM_s(t)I_T(t) \quad \text{(with speckle)} \quad . \tag{A-2}$$

To be physically meaningful, M_s must always be non-negative since S is the output of an optical detector. For this study we have limited our attention to modulation functions with an average value of unity over a typical COAT system convergence time (typically 1 to 2 msec). Since speckle is a wave-interference effect and consequently an energy-conserving

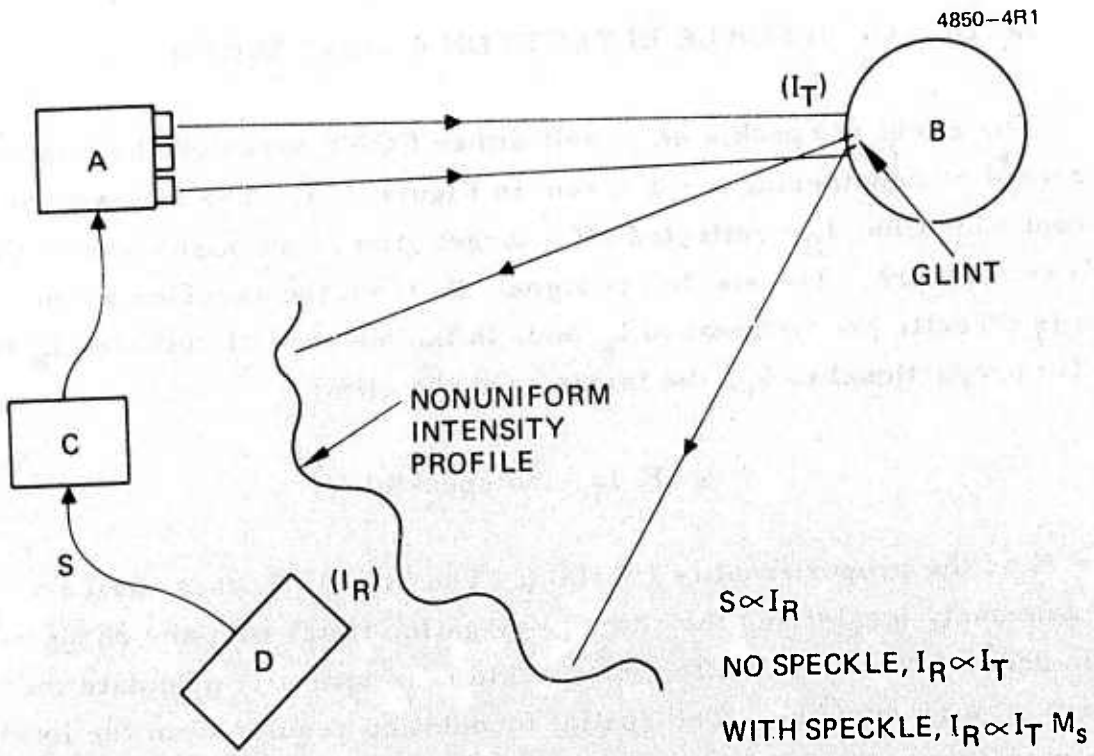

Figure A-1. Simple statement of the speckle problem
A: COAT laser array, B: Target,
C: COAT servo, D: Photomultiplier
receiver.

phenomenon, multiplying the intensity by M_s must not alter the total energy in the reflected radiation field. In other words the average energy incident on the receiver should be the same with or without the modulation function M_s. The intensity at the receiver is no longer required to be instantaneously proportional to the intensity on the target glint, but the average intensity at the receiver over a convergence time should still be proportional to the average intensity on the glint, and the constant of proportionality, K, in Eq. (A-2) should still be the same. Mathematically, this implies that the mean value or dc level of M_s must be unity.

Modulation functions with averages different from unity correspond physically to cases where the relative motion between the target and receiver are slow. In this case very few speckle lobes sweep across the receiver aperture during a convergence time. Consequently the speckle modulation frequencies are much lower than the dither frequencies and will not interfere with the convergence process. An automatic gain control (AGC) can be employed in the servo loop to remove these slow variations.

Subject to the above physically meaningful constraints, we define the otherwise completely arbitrary speckle modulation function,

$$M_s(t) \equiv \frac{1}{\sqrt{2\pi}} \int_{-\infty}^{\infty} d\omega \; a(\omega) \; e^{-i\omega t} \quad . \tag{A-3}$$

To aid in developing an analytical solution to the speckle problem, we will examine the nature of the signal S. We first separate I_T into two components,

$$I_T \equiv I_M + I_D + \left\{ \begin{matrix} \text{negligible} \\ \text{terms} \end{matrix} \right\} \simeq I_M + I_D \quad , \tag{A-4}$$

where I_M refers to the mean intensity and I_D refers to the dither modulations. A mathematical justification for Eq. (A-4) is given in the derivation of the statistical model in Section B (See Eqs. (A-11) and (A-12). Similarly,

we can separate M_s without approximations into a mean value or low frequency component M_M and a high frequency component M_{ac}.

$$M_s \equiv M_M + M_{ac} \tag{A-5}$$

Combining Eqs. (A-2), (A-4), and (A-5), we have

$$S = K\left[M_M I_M + M_M I_D + M_{ac} I_M + M_{ac} I_D + (\text{higher order terms})\right] . \tag{A-6}$$

The various filters and synchronous detectors in the COAT servo will pass signals only near the dither frequencies. Thus we need to consider only the terms $KM_M I_D$, containing the dither error information, and $KM_{ac} I_M$, containing the speckle induced interference at the dither frequencies. The rest of the terms contribute little or no signal in the dither band. The last term, $M_{ac} I_D$, is important only at very low covergence levels ($\lesssim 5\%$) which, as we shall show, are below any steady-state levels for the worst cases considered (see Section III of this report also). Our goal is to calculate the average power in both of these signals and then relate their power ratio to the COAT system convergence level. To do this, we must first develop a statistical model of a multidither COAT system.

B. STATISTICAL MODEL OF AN N-CHANNEL MULTIDITHER COAT SYSTEM

In order to derive a good statistical model, we begin by deriving the exact expression for the radiant intensity at a point (i.e., glint) on a distant target illuminated by an N-channel segmented COAT array. This system representation is perfectly general for the problem we are considering.

Consider the electric field of N separate waves having the same amplitude and wavelength incident on a given point (i.e., target glint).

Assume the polarization of each wave is adjusted so that they are all plane polarized parallel to each other. Then the total field, E_T, is

$$E_T(t) = \sum_{n=1}^{N} E_o \, e^{i\Gamma_n(t)} \qquad \text{(A-7)}$$

where E_o is the magnitude of each wave (assumed equal for each wave), and $\Gamma_n(t)$ is the time-varying phase of the n^{th} wave at the glint.

The radiant intensity, normalized to unity when all $\Gamma_n = 0$ (i.e., $E_o \equiv 1/N$), may be written as

$$I_T = \left|E_T\right|^2 = \frac{1}{N^2} \sum_{n=1}^{N} \sum_{m=1}^{N} \exp i\left[\Gamma_n(t) - \Gamma_m(t)\right] \quad . \qquad \text{(A-8)}$$

In a COAT multidither array, the N phase angles are physically dithered at different frequencies. For such an array, the phase in the n^{th} channel is $\Gamma_n(t) = \beta_n(t) + \psi \sin \omega_n t$. In this representation, $\beta_n(t)$ is a mean phase angle and ψ is the amplitude of the small dither deviation from the mean (typically $\psi < \pi/6$ radians). Substituting $\Gamma_n(t) = \beta_n(t) + \psi \sin \omega_n t$ into Eq. (A-8) we can expand the result in Bessel functions.

$$I_T = \frac{1}{N} + \frac{1}{N^2} \sum_{\substack{n=1 \\ n \neq m}}^{N} \sum_{m=1}^{N} e^{i(\beta_n - \beta_m)}$$

$$\left[\sum_{k=-\infty}^{\infty} J_k(\psi) \, e^{ik\omega_n t} \sum_{\ell=-\infty}^{\infty} J_\ell(-\psi) \, e^{i\ell\omega_m t} \right] \quad . \qquad \text{(A-9)}$$

Since we are only interested in the modulations at the dither frequencies and the overall convergence level, we need to consider only the first two terms in the Bessel expansions:

$$I_T = \frac{1}{N} + \frac{1}{N^2} \sum_{\substack{n=1 \\ n\neq m}}^{N} \sum_{m=1}^{N} \left\{ \cos(\beta_n - \beta_m) \left[J_o^2(\psi) + \ldots \right] \right.$$

$$+ \sin(\beta_n - \beta_m) \left[-2J_1(\psi)\, J_o(\psi) \left(\frac{e^{i\omega_n t} - e^{-i\omega_n t}}{2i} \right) \right.$$

$$\left. \left. + 2J_1(\psi)\, J_o(\psi) \left(\frac{e^{i\omega_m t} - e^{-i\omega_m t}}{2i} \right) + \ldots \right] \right\} . \qquad \text{(A-10)}$$

Thus we can identify I_M, the mean convergence level, and I_D, the modulations at the dither frequencies as:

$$I_M \equiv \frac{1}{N} + \frac{J_o^2(\psi)}{N^2} \sum_{\substack{n=1 \\ n\neq m}}^{N} \sum_{m=1}^{N} \cos(\beta_n - \beta_m) \quad , \qquad \text{(A-11)}$$

and

$$I_D \equiv - \frac{4J_o(\psi)\, J_1(\psi)}{N^2} \sum_{\substack{n=1 \\ n\neq m}}^{N} \sum_{m=1}^{N} \sin(\beta_n - \beta_m) \sin \omega_n t \quad . \qquad \text{(A-12)}$$

We thus have

$$I_T = I_M + I_D + \text{Higher order products of Bessel functions} \quad , \quad (A\text{-}4)$$

which is identical to Eq. (A-4). For small values of ψ, the higher order terms are negligible.

The convergence level and the dynamics of a COAT system are functions of N degrees of freedom, i.e., the N phase angles $\beta_1, \beta_2, \cdots \beta_N$. Given the value of each β and its time derivative at any instant of time, we can calculate the values of any dynamic variables of interest. The average or mean value, however, can be calculated quickly by using the following statistical model. Let a quasi-static or steady state convergence level be characterized by a random distribution of the phase angles β_1 through β_N over some interval α, as shown in Figure A-2. As α approaches zero, the COAT array will converge on the target glint (i.e., $I_T \rightarrow 1$ and thus $I_M \rightarrow 1$). Conversely, as α approaches 2π, the array approaches a minimum convergence level. The range of all possible relative phase differences, $\beta_m - \beta_n$, between any two channels, at a specified convergence level, is thus 0 to α. The probability density that a given $\beta_n = \beta$ is just $P(\beta) = \alpha^{-1}$ over this range and zero everywhere else. The probability density $P(\Delta\beta)$, for an arbitrary $\beta_m - \beta_n = \Delta\beta$, is the autocorrelation function of $P(\beta)$, given by:

$$P(\Delta\beta) = \frac{1}{a} - \frac{|\Delta\beta|}{a^2} \quad . \quad (A\text{-}13)$$

This expression holds in the region $-\alpha < \Delta\beta < \alpha$. Outside that region $P(\Delta\beta) \equiv 0$. This model allows us to calculate expectation values of various dynamic variables of particular interest for speckle effects such as the convergence level, $\langle I_M \rangle$, and the rms of the dither modulations, $\langle I_D^2 \rangle^{1/2}$.

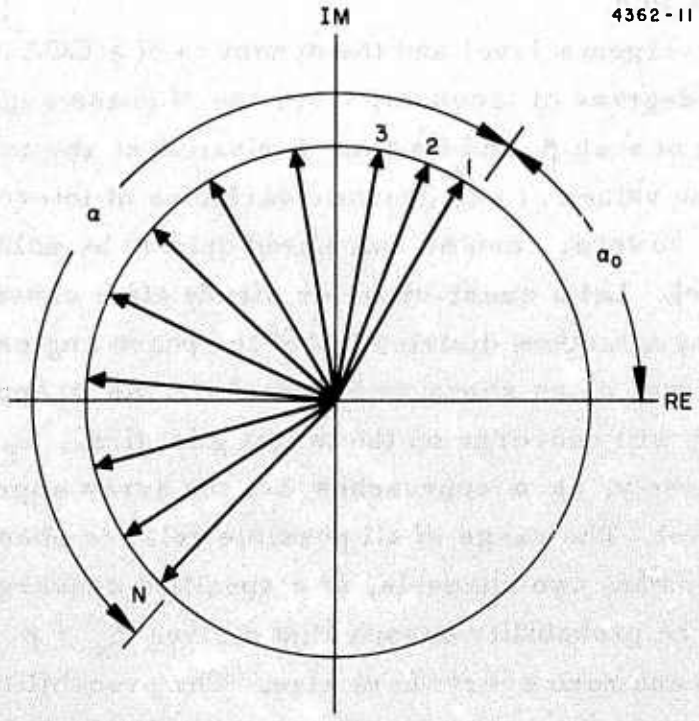

Figure A-2. Phaser diagram of a partially converged, N-element COAT array.

Using the definition of I_M in Eq. (A-10), we write the expectation value of I_M as:

$$\langle I_M \rangle = \frac{1}{N} + \frac{J_o^2(\psi)}{N^2} \sum_{\substack{n=1 \\ n \neq m}}^{N} \sum_{m=1}^{N} \langle \cos(\beta_n - \beta_m) \rangle \quad . \qquad (A-14)$$

Using Eq. (A-12), it is easy to show that

$$\langle \cos(\beta_n - \beta_m) \rangle = \int_{-\infty}^{\infty} P(\Delta\beta) \cos(\Delta\beta)\, d(\Delta\beta) = \frac{2}{\alpha^2}(1 - \cos\alpha) \quad . \qquad (A-15)$$

Thus we have

$$\langle I_M \rangle = \frac{1}{N} + J_o^2(\psi) \left(1 - \frac{1}{N}\right) \frac{2}{\alpha^2}(1 - \cos\alpha) \quad . \qquad (A-16)$$

Figure A-3 shows a plot of $\langle I_M \rangle$, versus α for an 18-element array, and a peak dither amplitude of $\psi = 0.349$ radians (20^o).

A similar calculation using Eq. (A-12) shows that $\langle I_D \rangle = 0$, and

$$\langle I_D^2 \rangle = \frac{1}{2}\left(\frac{4J_o(\psi)\, J_1(\psi)}{N^2}\right)^2 \sum_{n=1}^{N} \left\langle \left[\sum_{\substack{m=1 \\ m \neq n}}^{N} \sin(\beta_n - \beta_m) \right]^2 \right\rangle \quad . \qquad (A-17)$$

In Eq. (A-17) we ignore the additional oscillatory terms at frequencies $\omega_n + \omega_m$ and $\omega_n - \omega_m$ because of the assumed quasi-static steady state where the convergence level remains fairly constant over a long period of time. These terms will therefore have a time average close to zero. Let

$$b_n \equiv \sum_{\substack{m=1 \\ n \neq m}}^{N} \sin(\beta_n - \beta_m) \quad . \qquad (A-18)$$

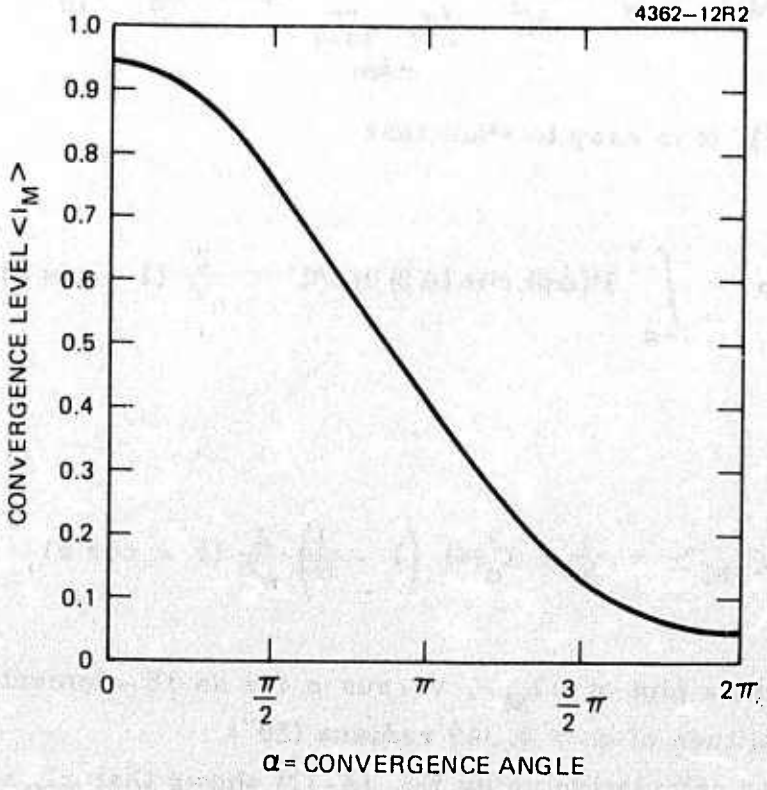

Figure A-3. Statistical expectation value of the convergence level versus α for an 18-channel multidither COAT system (dither amplitude = 20°), calculated from eq. 16.

Since b_n is a function of the random variables $\beta_1, \beta_2, \ldots, \beta_N$, it is also a random variable whose expectation value is expressed as

$$\langle b_n^2 \rangle = \int d\beta_1 \int d\beta_2 \cdots \int d\beta_N \, P(\beta_1) \, P(\beta_2) \cdots P(\beta_N) \, b_n^2 (\beta_1, \beta_2 \cdots \beta_N) \quad . \tag{A-19}$$

We have assumed that the β's are randomly distributed between the phase angles α_o and $\alpha_o + \alpha$ as indicated in Figure A-2. Since α_o is arbitrary, it will be convenient to define it as a $\alpha_o \equiv -\alpha/2$; this will make the integrals in Eq. (A-9) easier to calculate. Using the above information plus the definition of b_n in Eq. (A-18) we can rewrite Eq. (A-19).

$$\langle b_n^2 \rangle = \alpha^{-3} \sum_{\substack{m=1 \\ m \neq k, n \\ k \neq n}}^{N} \sum_{k=1}^{N} \int_{-\alpha/2}^{\alpha/2} d\beta_m \int_{-\alpha/2}^{\alpha/2} d\beta_K \int_{-\alpha/2}^{\alpha/2} d\beta_n \sin(\beta_n - \beta_m) \sin(\beta_n - \beta_k)$$

$$+ \alpha^{-2} \sum_{\substack{m=1 \\ m \neq n}}^{N} \int_{-\alpha/2}^{\alpha/2} d\beta_m \int_{-\alpha/2}^{\alpha/2} d\beta_n \sin^2(\beta_n - \beta_m) \tag{A-20}$$

Carrying out the integrals gives

$$\langle b_n^2 \rangle = \frac{1}{2}(N^2 - 3N + 2) \frac{\sin^2\left(\frac{\alpha}{2}\right)}{\left(\frac{\alpha}{2}\right)^2} \left[1 - \frac{\sin\alpha}{\alpha}\right] + \frac{1}{2}(N-1)\left[1 - \frac{\sin^2\alpha}{\alpha^2}\right] \quad . \tag{A-21}$$

Substitution of Eqs. (A-18) and (A-21) into Eq. (A-17) gives

$$\langle I_D^2 \rangle = 4\left[J_o(\psi)\, J_1(\psi)\right]^2 \left\{ \left(\frac{1}{N} - \frac{3}{N^2} + \frac{2}{N^3}\right) \frac{\sin^2\left(\frac{\alpha}{2}\right)}{\left(\frac{\alpha}{2}\right)^2} \left[1 - \frac{\sin\alpha}{\alpha}\right] \right.$$

$$\left. + \left(\frac{1}{N^2} - \frac{1}{N^3}\right)\left[1 - \frac{\sin^2\alpha}{\alpha^2}\right] \right\} \quad . \qquad \text{(A-22)}$$

The rms dither amplitude is just the square root of Eq. (A-20). A plot of the rms dither amplitude versus α for an 18-element COAT array with $\psi = 0.349$ rad (20^o) is shown in Figure A-4. Since α is just a statistical parameter, it is more meaningful to plot the dither amplitude as a function of the convergence level, $\langle I_M \rangle$ as shown in Figure A-5.

C. PREDICTIONS OF EQUILIBRIUM CONVERGENCE LEVELS

At this point, we make an assumption about the convergence of a COAT system. Later we will verify the assumption with computer simulation data. The assumption is that the COAT array will converge to an equilibrium level where the average power in the synchronously detected dither signals, P_D, is equal to the average power in the synchronously detected speckle induced signals, P_S. During the original development of this analysis, we chose to calculate the average power in these two signals before synchronous detection. It is just as easy to do the analysis this way as long as we recognize that the detection process alters the relative power in these signals. This alteration happens because the phases of the synchronous detectors are synchronized to the dither phases while the speckle induced modulations are random. The detection process thus introduces a time averaging into the speckle signal which does not occur in the dither signal. The net result is a factor of 2 increase in the power ratio.

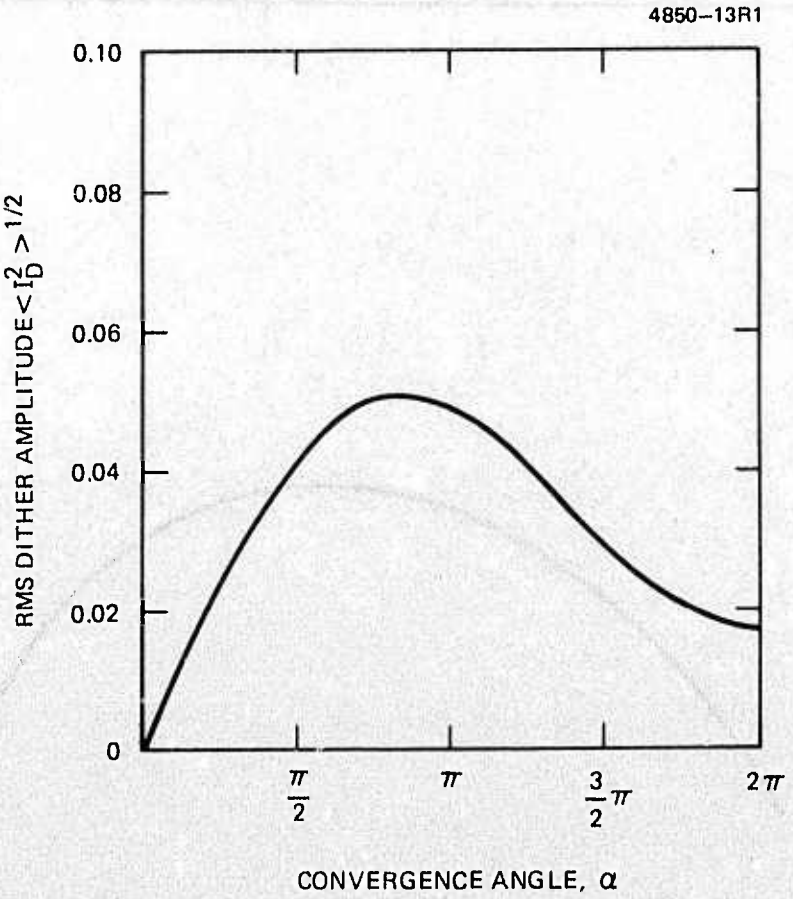

Figure A-4. Statistical expectation value of the rms dither amplitude versus α for an 18-channel multidither COAT system (dither amplitude = 20°).

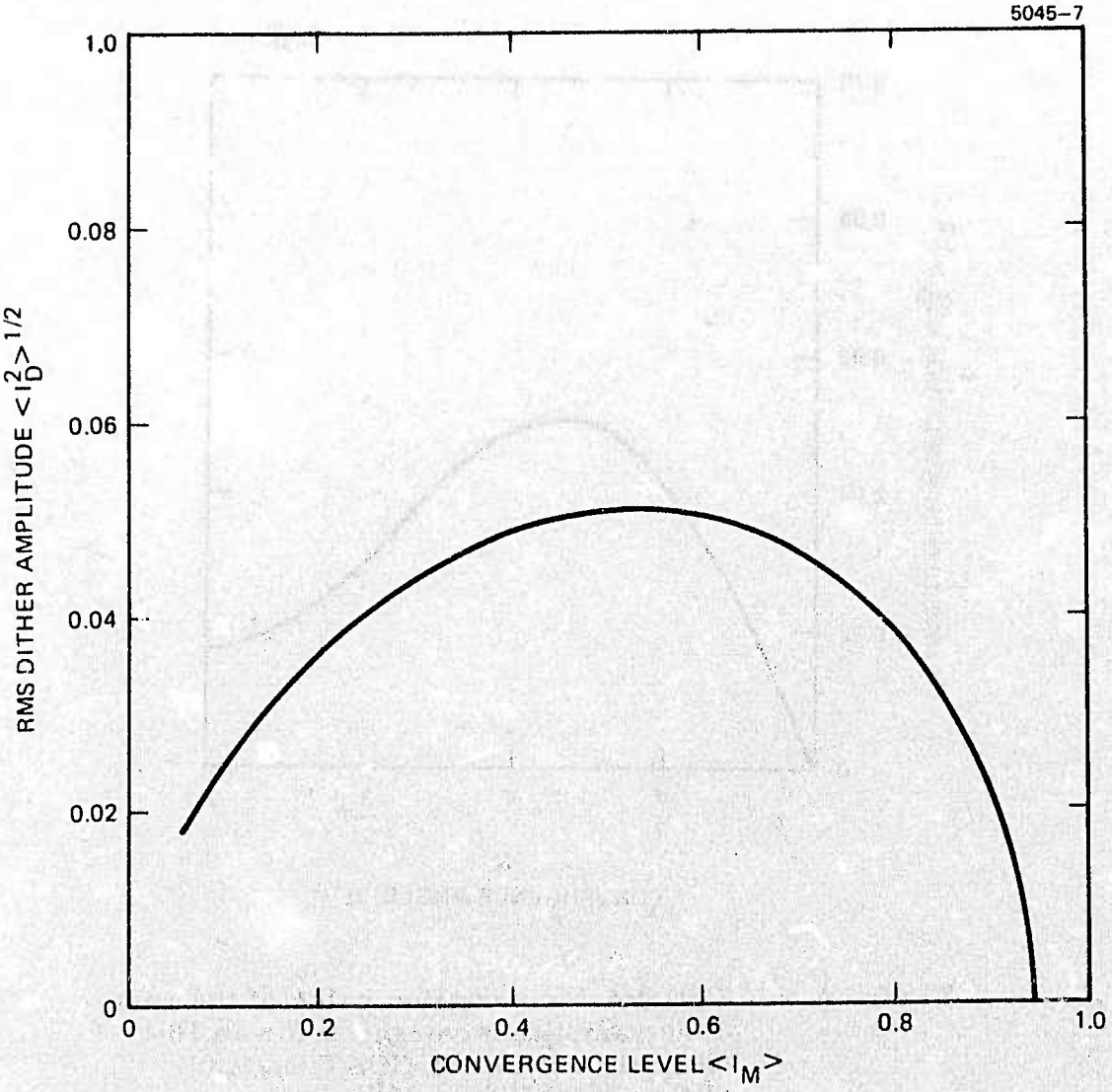

Figure A-5. Statistical expectation value of the rms dither amplitude versus convergence level for an 18-channel multidither COAT system (dither amplitude = 20°).

If we define the power ratio, ρ, before synchronous detection

$$\rho = \frac{\langle P_D \rangle}{\langle P_S \rangle} \tag{A-23}$$

then we can define, ρ', the power ratio after synchronous detection as: $\rho' = 2\rho$. Thus the equilibrium convergence level will correspond to that level where $\rho = 0.5$. We now proceed to calculate this predicted convergence level.

Let S_D be that portion of the signal S containing the dither error signal:

$$S_D = K M_M I_D \quad . \tag{A-24}$$

The expectation value of the average power at the dither frequencies is

$$\langle P_D \rangle = \frac{1}{2T} \int_T^T \langle S_D^2 \rangle \, dt$$

$$= \frac{K^2}{2T} \int_{-T}^{T} \langle I_D^2 \rangle \langle M_M^2 \rangle \, dt = K^2 \langle I_D^2 \rangle \quad , \tag{A-25}$$

where we have used $\langle M_M^2 \rangle \simeq \langle a(0)^2 \rangle = 1.0$. Let S_S be that portion of the signal S in the term $KM_{ac}I_M$ which causes spurious modulations near the dither frequencies. In order to calculate this signal, we define a "speckle coefficient," C_S, as

$$C_S \equiv \left\{ \sum_{\pm\omega_i} \int_{\omega_i - \Delta\omega}^{\omega_i + \Delta\omega} \frac{a(\omega) a^*(\omega)}{2T} \, d\omega \right\}^{1/2} \tag{A-26}$$

This coefficient is the square root of the sum of 2N integrals, where N is the number of dither frequencies in the COAT servo. The summation is carried out over both positive and negative values of the dither frequencies, ω_i. The quantity $\Delta\omega$ is the open loop, unity-gain bandwidth of each COAT servo channel. These quantities are shown graphically in Figure A-6 for the positive half of the power spectrum of an arbitrary modulation function. The shaded area corresponds to the integrals in Eq. (A-26).

Physically, C_s^2 corresponds to that portion of the ac modulation power in M_s which is at or near enough to each dither frequency so that it can create false error signals which compete with the correct dither signals for control of the convergence process. Thus the average power in the signal S_S is given by

$$\left\langle P_S \right\rangle = \frac{1}{2T} \int_{-T}^{T} \left\langle S_S^2 \right\rangle dt = K^2 \left\langle I_M^2 \right\rangle C_S^2 \quad . \quad \text{(A-27)}$$

The quantity C_S has the interesting property that it is never larger than 0.707. This can be understood by considering the total average power, P_{TS}, of the speckle modulation function M_s:

$$P_{TS} = \lim_{T \to \infty} \frac{1}{2T} \int_{-T}^{T} M_s(t)\, M_s(t)^* \, dt \qquad \text{(A-28)}$$

Using the definition of $M_s(t)$ in Eq. (A-3) gives:

$$P_{TS} = \lim_{T \to \infty} \frac{1}{2T} \int_{-\infty}^{\infty} a(\omega)\, a^*(\omega)\, d\omega \qquad \text{(A-29)}$$

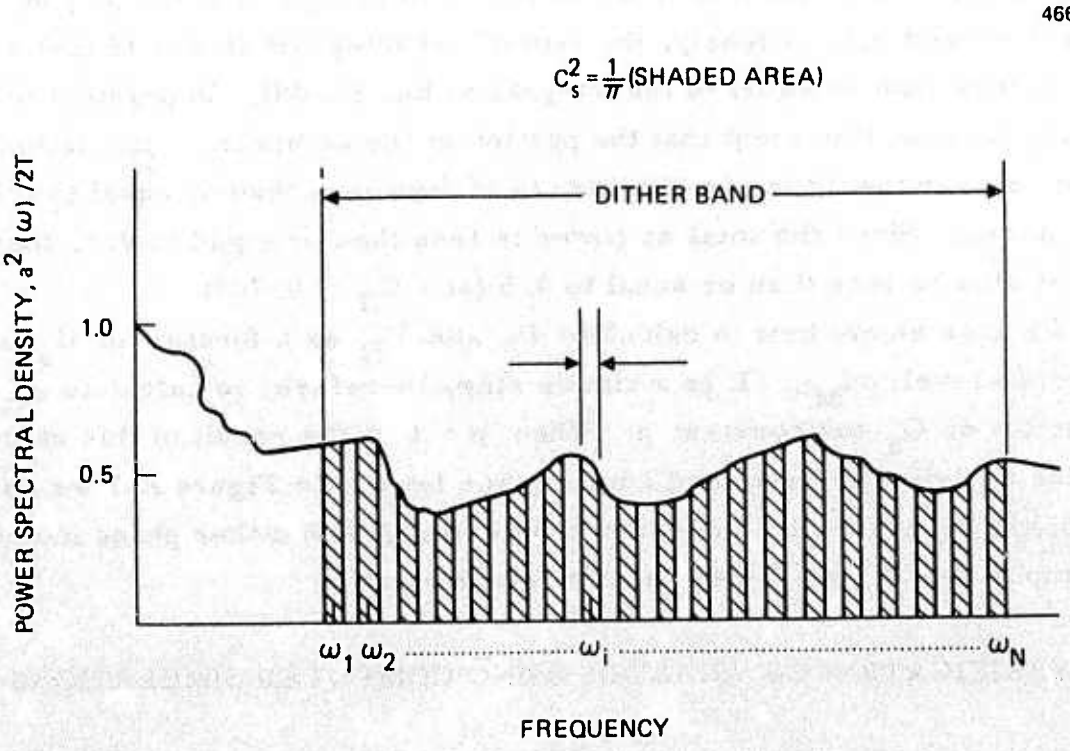

Figure A-6. Power spectrum of an arbitrary modulation function.

A limiting value for P_{TS} occurs when M_s consists of a unit dc level and a unit amplitude single frequency modulation. In this case $P_{TS} = 1.5$. A more realistic modulation function would include many frequencies with random phases. The requirements that M_s must always be non negative and have an average value of 1.0 however, prevents P_{TS} from exceeding this limiting value. Furthermore, if the dc power is always 1.0, the ac power will never exceed 0.5. Clearly, the sum of the integrals in Eq. (A-26) will always be less than or equal to the integral in Eq. (A-29). In physical terms, this is the obvious statement that the portion of the ac speckle modulation power at or near the dither frequencies is always less than or equal to the total ac power. Since the total ac power is less than or equal to 0.5, then C_s^2 must also be less than or equal to 0.5 (and $C_S \leq 0.707$).

We have shown how to calculate P_S and P_D as a function of C_s and convergence level, $<I_M>$. It is a simple step, therefore, to calculate $<I_M>$ as a function of C_s for constant ρ. When $\rho = 0.5$ the result of this calculation is the analytically predicted convergence level. In Figure A-7 we show the predicted level for an 18-element COAT array with dither phase modulation amplitudes of $\psi = 0.349$ radians (20 degrees).

D. VERIFICATION OF ANALYSIS USING COMPUTER SIMULATIONS

Computer simulations have verified that the analytical approach described above gives very accurate predictions of average convergence levels, provided the servo bandwidth variation with convergence level can be ignored. In a typical COAT servo, the gain in each channel is a function of all the phases in the N channels; i.e., the gain is a function of the overall system convergence level and the phase error in that channel. But since the servo bandwidth is a function of the gain, it also varies with the overall convergence level and the phase error in that channel. Typically, the bandwidth in all channels is small at low convergence levels and increases to a maximum value at full convergence for a servo without an AGC. When a divider AGC is included in the loop, variation in gain and thus bandwidth from channel to channel is very large at low convergence levels and then approaches a constant, generally lower level in all channels at full convergence. This dependence of servo bandwidth on convergence level makes a straightforward

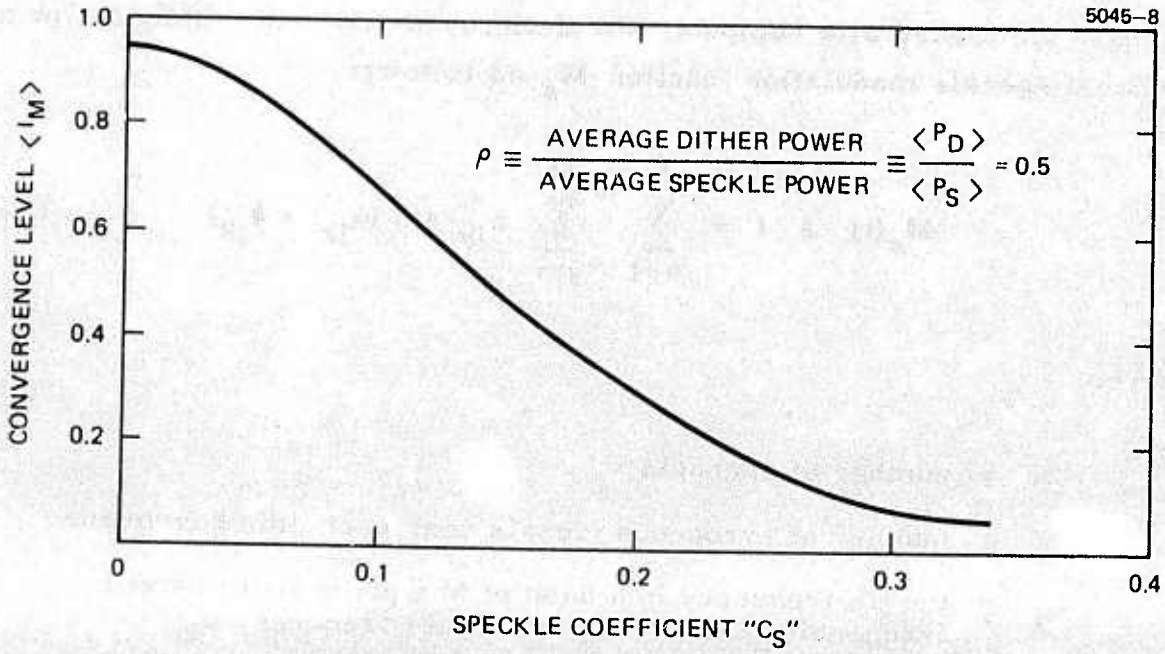

Figure A-7. Analytically predicted convergence level and an 18-channel COAT array (dither amplitude = 20°).

analytical prediction of convergence level somewhat more difficult because the servo bandwidth must be known to calculate C_s. The equilibrium convergence level is then found as shown from Figure A-7. The servo bandwidth associated with this predicted level, however, may not be the same as the bandwidth originally chosen to calculate C_s. Thus, several iterative calculations are necessary to insure that all these parameters are compatible with each other.

In order to avoid these iterative calculations and still be able to compare the theory with computer simulations, we can alternately define an artificial speckle modulation function M_s as follows:

$$M_s(t) \equiv 1 + \sum_{k=1}^{N} \sum_{j=1}^{M} a_{jk} \sin(\omega_{jk} t + \phi_{jk}) \qquad (A\text{-}27)$$

where:

$N \equiv$ number of channels

$M \equiv$ number of erroneous signals near each dither frequency

$\omega_{jk} \equiv$ the jth frequency in a band of M equally incremented frequencies centered at the dither frequency ω_k

$\phi_{jk} \equiv$ a randomly chosen phase angle between 0 and 2π

$a_{jk} \equiv$ a randomly chosen amplitude between 0 and an adjustable maximum, a_{max}.

The ω_{jk} are chosen to lie in a sufficiently narrow band around each dither frequency so that the servo bandwidth is always larger than this band at all convergence levels. A speckle coefficient C_s that is effectively independent of servo bandwidth can then be calculated and the resulting analytically predicted convergence levels can be compared to a computer simulation run which uses an identical modulation function. In this study we chose 21 equally spaced frequencies over a bandwidth of ±83 Hz around each of 18 dither frequencies (i.e., N = 18, M = 21). By choosing different values for a_{max}, we were able to gather data for different values of C_s ($C_s \approx 8\, a_{max}$).

Simulations were run at three values of broadband signal-to-noise ratio (receiver shot noise): 10^{10}, 40, and 20. When $(S/N)_{shot} = 10^{10}$ and $C_s = 0$ (no speckle noise), the simulation produces a time history of the convergence level, or intensity on the target glint as shown in Figure A-8(a). When the speckle noise modulation shown in Figure A-8(c) is present ($C_s = 0.127$), the time history in Figure A-8(b) results.

The behavior shown in Figure A-8(b) for $C_s \neq 0$ is typical. In general, the speckle modulations have two effects: (1) the mean convergence level is lowered; and (2) a random oscillation of the intensity occurs between a maximum convergence level and a minimum level. This oscillation is much slower than the dither oscillations (on the order of 0.5 to 1.0 kHz versus 10.0 to 40.0 kHz) and its magnitude varies with convergence level. Figure A-9 shows a plot of the maxima and minima recorded during these simulations as a function of C_s.

Also shown in Figure A-9 is the analytically predicted mean convergence level corresponding to $\rho = 0.5$ and two other analytical curves corresponding to $\rho = 0.25$ and $\rho = 1.0$. Notice that the maximum and minimum convergence levels correspond very well to these two values of ρ. In terms of the power ratio after demodulation, ρ', we see that $\rho' = 1$ corresponds to the mean convergence level, $\rho' = 0.5$ corresponds to the maximum level, and $\rho' = 2$ corresponds to the minimum level. Evidently when the relative power in the dither signal after demodulation is a factor of 2 greater than the speckle signal, it will totally dominate and the COAT system will converge; conversely, when the power in the speckle signal is a factor of two greater than the dither signal it will totally dominate and the COAT system will fail to converge any further.

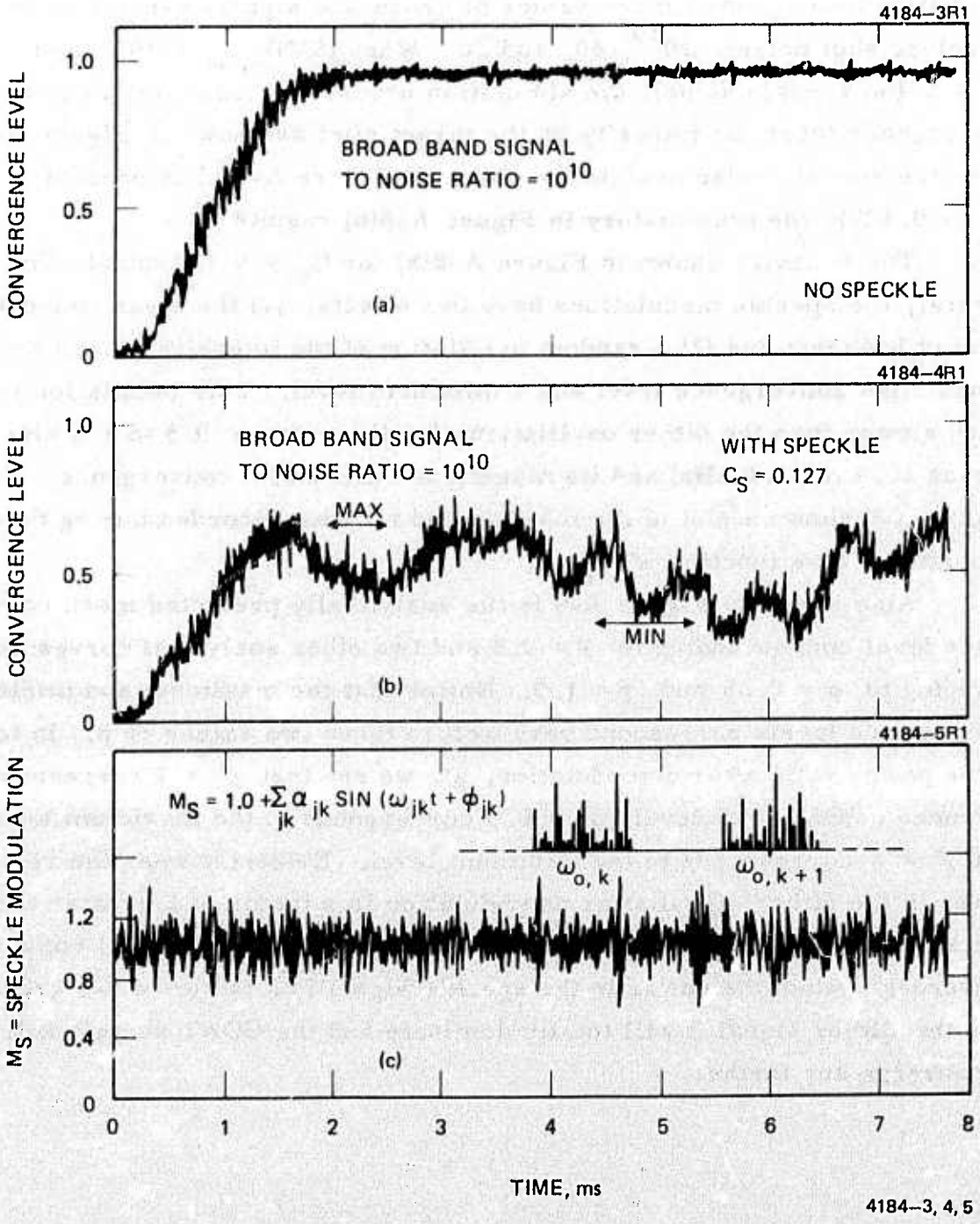

Figure A-8. Typical time histories from computer simulations. Signal to noise ratio = 10^{10}. (a) COAT performance with no speckle, $C_s = 0.0$. (b) COAT performance with speckle, $C_s = 0.127$. (c) Speckle modulation function used to produce (b).

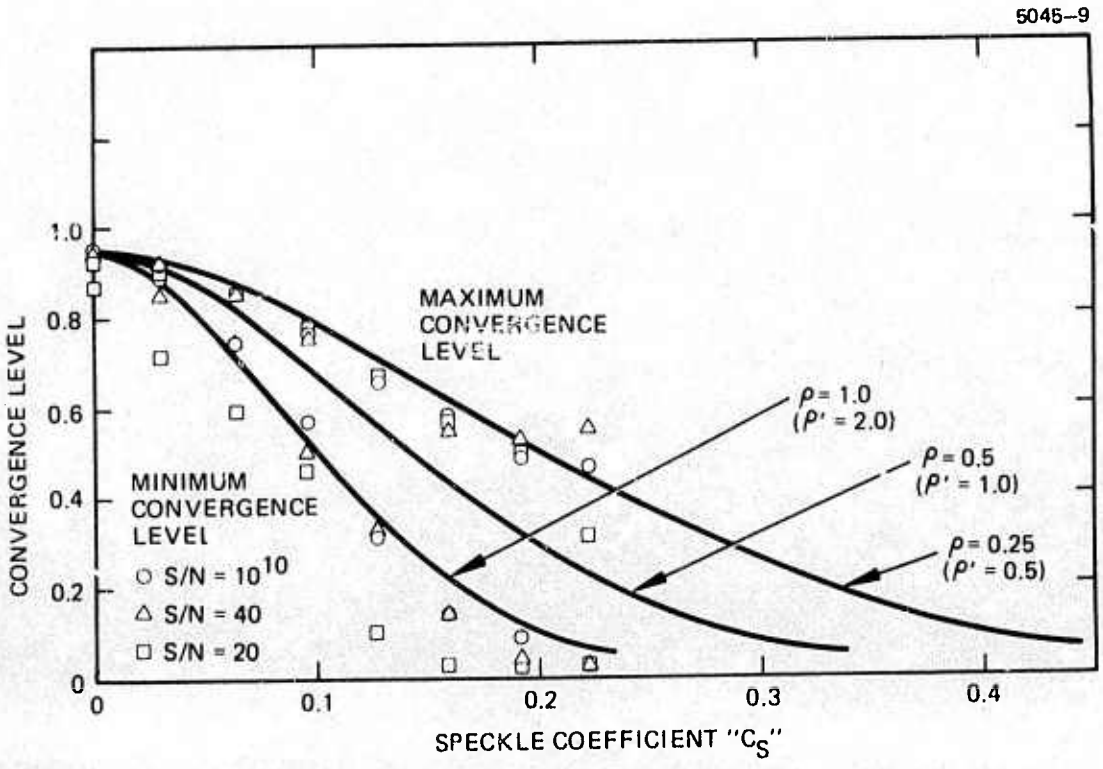

Figure A-9. Convergence level versus C_s theory and computer simulation data for an 18-channel COAT array (20^o dither amplitude).

APPENDIX B

SYSTEM SAFETY ANALYSIS

Paragraph 4.4 of the contract statement of work requires that a system safety analysis be performed in accordance with paragraph 5.8.2.1 of MIL-STD-882. Such an analysis was performed during the course of the contract work to identify, and correct where necessary, possible hazards associated with the operation of the system known as the "multidither COAT experimental model" (hereafter called "the COAT system") used in the experimental tasks of this contract. The analysis performed follows a similar analysis* performed for the same COAT system when it was located in a different area.

There are two potential hazard sources for users of this system within the laboratory environment where this contract work was performed: (1) electrical shock and (2) eye damage by laser radiation. Appropriate safety precautions have been taken as part of the Hughes Industrial Safety Program to insure sufficient fire protection, clearance for egress from the laboratory, access to power line breakers, etc., so that the requirements of the California OSHA codes are satisfied.

Electrical shock from the COAT system was assessed to be in Category I – Negligible as defined in paragraph 3.14 of MIL-STD-882. Proper design of the electrical parts of the system insures that no personnel can encounter lethal or hazardous electrical voltage and/or current levels.

The hazard level for optical eye damage was assessed to be in Category II – Marginal. The nature of the program required working with two laser sources, a 30 mW He-Ne unit operating at 0.6328 μm and a 1.5 W argon unit with an output wavelength of 0.488 μm. Various system optics reduce the maximum potential power levels to 10 mW at 0.6328 μm and 100 mW at 0.488 μm. The potential hazard is adequately controlled by providing safety glasses for all personnel while working on or around the system and by using masks, optical stops, etc. to confine the optical laser beams to

---

*W.B. Bridges, et al., RADC-TR-74-108, Jan. 1974, Contract F30602-73-C-0248, (779668).

areas where no personnel can directly view them at day point where the optical power density exceeds 2.5 mW/cm^2.

Sufficient safety procedures have thus been implemented to insure that both the 0.6328 μm radiation (a Class III hazard at the laser output) and the 0.488 μm radiation (a Class IV hazard at the laser output) are adequately controlled to reduce the hazard to Category II for personnel working within the laboratory where the COAT system is operated. In addition, personnel are instructed in proper safety procedures while within the laboratory. Appropriate warning signs notify visitors to the laboratory and laser safety goggles are available for visitors.

MISSION
of
Rome Air Development Center

RADC plans and conducts research, exploratory and advanced development programs in command, control, and communications (C^3) activities, and in the C^3 areas of information sciences and intelligence. The principal technical mission areas are communications, electromagnetic guidance and control, surveillance of ground and aerospace objects, intelligence data collection and handling, information system technology, ionospheric propagation, solid state sciences, microwave physics and electronic reliability, maintainability and compatibility.